

STATE OF ARKANSAS

ARKANSAS GEOLOGICAL SURVEY
BEKKI WHITE, STATE GEOLOGIST

MISCELLANEOUS PUBLICATION 23

**THERMAL CONDUCTIVITY, THERMAL GRADIENT, AND HEAT
FLOW ESTIMATIONS FOR THE SMACKOVER FORMATION,
SOUTHWEST ARKANSAS**

By

Lea Nondorf

2023 Edits by Ciara Mills



Little Rock, Arkansas

2013

STATE OF ARKANSAS

ARKANSAS GEOLOGICAL SURVEY
BEKKI WHITE, STATE GEOLOGIST

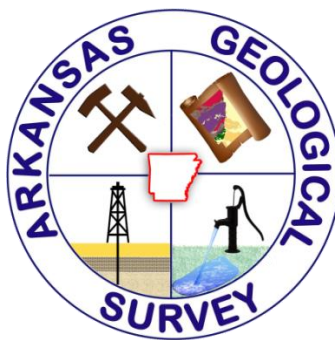
MISCELLANEOUS PUBLICATION 23

**THERMAL CONDUCTIVITY, THERMAL GRADIENT, AND HEAT
FLOW ESTIMATIONS FOR THE SMACKOVER FORMATION,
SOUTHWEST ARKANSAS**

By

Lea Nondorf

2023 Edits by Ciara Mills



Little Rock, Arkansas

2013

STATE OF ARKANSAS

Mike Beebe, Governor

Arkansas Geological Survey

Bekki White, Director and State Geologist

Commissioners

| | |
|--|--------------|
| Dr. Richard Cohoon, Chairman..... | Russellville |
| Mr. William Willis, Vice Chairman..... | Hot Springs |
| Mr. Quin Baber III..... | Benton |
| Mr. William Cains, Sr..... | Altus |
| Mr. Ken Fritsche..... | Greenwood |
| Mr. Gus Ludwig..... | Quitman |
| Mr. David Lumbert..... | Little Rock |

Little Rock, Arkansas

2013

Table of Contents

| | |
|--|----|
| Abstract..... | 1 |
| Introduction..... | 1 |
| Smackover Formation Description | 2 |
| Geothermal Energy | 3 |
| Geothermal Power Plants..... | 3 |
| Previous Smackover Geothermal Studies..... | 6 |
| Possible Explanation of High Subsurface Temperatures in South Arkansas. | 6 |
| Thermal Conductivity | 6 |
| Smackover Thermal Conductivity Sampling Method. | 6 |
| Thermal Conductance Correction for <i>In Situ</i> Conditions. | 10 |
| Thermal Conductance Results. | 16 |
| Thermal Gradient..... | 16 |
| Correcting for <i>In Situ</i> Borehole Temperatures Using the Harrison Correction Equation.... | 18 |
| Determining Estimated Geothermal Gradients for Southwest Arkansas..... | 18 |
| Corrected Geothermal Gradient Results and Comparison..... | 18 |
| Heat Flow..... | 22 |
| Calculating Geothermal Heat Flow. | 22 |
| Discussion of Estimated Heat Flow Maps..... | 22 |
| Verification of Data | 27 |
| Conclusion | 30 |
| References..... | 31 |
| Appendices..... | 34 |

Figures

| | |
|--|----|
| Figure 1. General stratigraphic chart of the subsurface Jurassic section indicating relative stratigraphic position of the Smackover Formation, south Arkansas. | 2 |
| Figure 2. Isopach contours of top of Smackover Formation. | 4 |
| Figure 3. Structural contours of top of Smackover Formation. | 5 |
| Figure 4. Locations of sampled core from wells in southern Arkansas..... | 8 |
| Figure 5. KD2 Pro Thermal Analyzer device showing probe inserted into core of interbedded anhydrite in dolostone..... | 9 |
| Figure 6. Hilti rotary hammer used for core sample drilling. | 9 |
| Figure 7. Oolitic grainstone of the upper Smackover Formation | 13 |
| Figure 8. Oolitic to pisolitic crystalline limestone of the upper Smackover Formation..... | 14 |
| Figure 9. Oolitic grainstone exhibiting oomoldic porosity | 14 |
| Figure 10. Average thermal conductance values for each Smackover well in W/m·K..... | 15 |
| Figure 11. Geothermal gradient ranges for each of the Smackover Formation in °C/100m. ... | 20 |
| Figure 12. Geothermal gradient raster image of the Smackover Formation in °C/100m..... | 21 |
| Figure 13. Estimated heat flow for each Smackover Formation well in mW/m ² | 23 |
| Figure 14. Estimated heat flow map of southwestern Arkansas..... | 24 |
| Figure 15. Estimated heat flow contour map of the Smackover Formation | 25 |
| Figure 16. Southern Methodist University (SMU) heat flow data from southwest Arkansas for comparison with heat flow data generated by the AGS | 26 |
| Figure 17. Estimated heat flow map of southwestern Arkansas with recalculated average heat flows | 28 |
| Figure 18. Estimated heat flow contour map of the Smackover Formation with recalculated average heat flows | 29 |

Tables

| | |
|---|----|
| Table 1. Smackover thermal conductance results..... | 11 |
| Table 2. Comparing published thermal conductance values (W/m·K) with AGS thermal conductance values for varying lithologies..... | 17 |
| Table 3. Harrison correction, corrected temperature, and estimated average geothermal gradient values for 18 Smackover wells in southwest Arkansas..... | 19 |

Appendices

| | |
|---|----|
| Appendix 1. Results of the 10 non-Smackover wells..... | 34 |
| Appendix 2. Additional photographs of Smackover Formation core samples..... | 36 |
| Appendix 3. Harrison Correction, corrected temperatures, and geothermal gradient values for 10 non-Smackover wells..... | 38 |

Abbreviations

| |
|--|
| AGS-Arkansas Geological Survey |
| AOGC-Arkansas Oil and Gas Commission |
| AP&L-Arkansas Power and Light Company (now Entergy Operations, Inc.) |
| BHT-Borehole Temperature |
| DOE-Department of Energy |
| EGS-Enhanced Geothermal Systems |
| GEA-Geothermal Energy Association |
| NGDS-National Geothermal Data System |
| PEDBs-Portable Electronic Divided Bars |
| SMU-Southern Methodist University |
| UND-University of North Dakota |

Acknowledgments

This publication was written to provide geothermal results generated by the Arkansas Geological Survey for the State Geothermal Data Project, sponsored by the U.S. Department of Energy under prime award number DE-EE0002850, awarded to the State of Arkansas under sub award number AR-EE002850. I would like to thank Corbin Cannon for helping to collect, drill, and measure core samples, Jason Tipton for providing well log and core information and for assisting me in generating the raster maps, and the AGS staff for helping with the editing of this manuscript.

Note on 2023 edits: it was brought to our attention that the total depth (TD) value for a well in Table 3 (Permit 24227) was incorrect in the original 2013 publication, leading to exaggerated geothermal gradient and heat flow calculations for this well. Figures, tables, and text have been updated to reflect the correct values.

THERMAL CONDUCTIVITY, THERMAL GRADIENT, AND HEAT FLOW ESTIMATIONS FOR THE SMACKOVER FORMATION, SOUTHWEST ARKANSAS

By

Lea Nondorf

Abstract

Subsurface thermal conductivity, thermal gradient, and heat flow are significant parameters when determining the feasibility of utilizing a geologic unit to generate industrial geothermal power. Core samples from 18 wells of the subsurface Jurassic Smackover Formation in southwest Arkansas were analyzed at the Arkansas Geological Survey where estimated thermal conductivity, thermal gradient, and heat flow values were determined. Thermal conductance of several samples was obtained using a KD2 Pro Thermal Analyzer at room temperature. Thermal gradients were estimated from Smackover borehole temperatures, and estimated heat flow was calculated from thermal conductance and thermal gradient values. Average estimated thermal conductance values for the Smackover Formation are greatest in northeastern Lafayette County at 2.57 Watts per meter Kelvin, or $W/m \cdot K$, followed by southern Columbia and western Calhoun Counties at 2.47 $W/m \cdot K$ each. Southern Columbia, southern Nevada, and western Calhoun Counties exhibit the highest estimated thermal gradient and heat flow with values greater than $3.3^{\circ}C/100m$ and 70 milliWatts per meter per meter, or mW/m^2 , respectively. Interpretation of these parameters suggests that these areas exhibit the highest geothermal potential for the Smackover Formation in southwest Arkansas. Investigations further characterizing the Smackover Formation, including *in situ* thermal properties and borehole temperature measurements, are recommended for future geothermal feasibility studies.

Introduction

Worldwide interest in renewable energy resources has created a need for more data to help determine the feasibility of developing these energy alternatives. Geothermal energy is one potential resource which is currently being evaluated by each state in participation with the State Geothermal Data Project, a collaborative project organized by the Association of American State Geologists (AASG) and funded by the Department of Energy (DOE). The Arizona Geological Survey, under the direction of Lee Allison, was designated by the AASG to collect and contribute digitized legacy geothermal data from all 50 states to the National

Geothermal Data System (NGDS), a publicly available database network. The Arkansas Geological Survey (AGS) contributed geothermal data primarily from the Smackover Formation in southern Arkansas in the form of borehole temperatures (BHT's), drillers' logs, earthquake hypocenters, geothermal-relevant documents, and thermal conductance measurements (available at <http://services.usgin.org/track/report/AR>). Observed high temperature data of the Smackover Formation prompted further investigation into its potential as a geothermal reservoir for the state.

The purpose of this manuscript is to characterize the subsurface thermal

conductivity, thermal gradient, and heat flow of the Smackover Formation as a potential geothermal energy resource in southwest Arkansas. The data was collected over a two-year period starting in 2010.

Smackover Formation Description

In southern Arkansas, the Upper Jurassic (Oxfordian, 161-156 Ma) Smackover Formation, named after the Smackover Field, Union County, Arkansas (Figure 1), was one of the first major oil producing units in the state. The Smackover contributed hundreds of millions of barrels of oil and condensate during early stages of production in the late 1930's to late 1940's (Vestal, 1950). The Smackover Formation is informally divided into the upper and lower Smackover.

The upper Smackover Formation was the major hydrocarbon producer in southern Arkansas, primarily from the Reynolds oolite (where present). The upper section consists mostly of a white to brown, porous oolitic to pisolitic grainstone with local inclusions of calcite, pyrite, anhydrite, gypsum, and lignite (Vestal, 1950). Sucrosic texture is also common as a secondary feature generated from the weathering of oolites and/or pisolites (Vestal, 1950). Bromine brines are associated with the upper Smackover in south Arkansas. A *Mining Engineering* journal (Ober, 2012) reports all U.S. bromine was recovered from the bromine-rich brines of the Smackover Formation in Arkansas and is the state's leading mineral commodity.

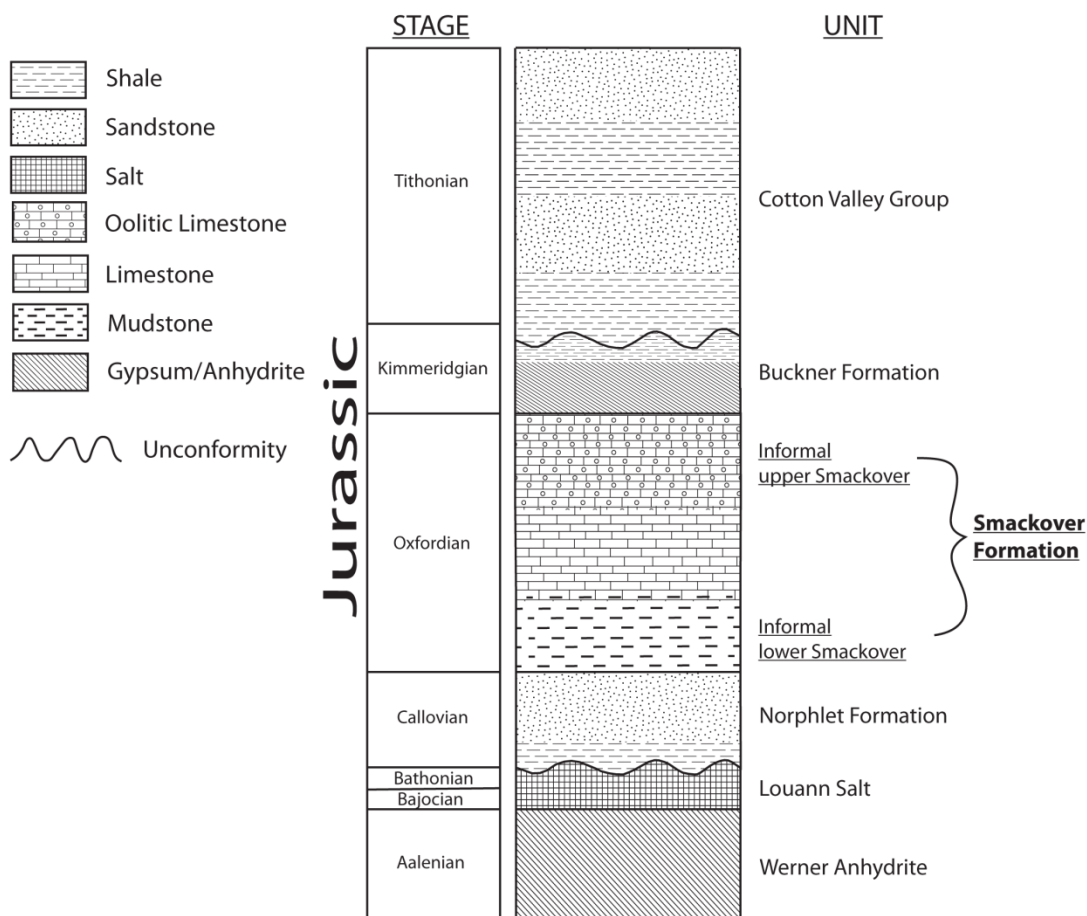


Figure 1. General stratigraphic chart of the subsurface Jurassic section indicating relative stratigraphic position of the Smackover Formation, south Arkansas.

The informal lower Smackover is the source rock for petroleum present in the informal upper Smackover as well as some Cretaceous reservoirs. Because of the development of new drilling technologies, several oil and gas companies are currently exploring the economic potential of the lower Smackover, or Brown dense, as a commercial and unconventional reservoir. The lower section is described as an organic-rich, very dense, dark-brown, very fine-grained, calcareous mudstone (Weeks, 1938).

The Smackover thins and eventually disappears near its northernmost edge (Figure 2). Structural contours on the top of the Smackover Formation show the unit ranges from a depth of 1,000 ft (305 m) near its northernmost boundary to approximately 11,000 ft (3,353 m) in extreme southwestern Arkansas (Figure 3).

Geothermal Energy

Geothermal energy is thermal energy stored within Earth's crust and is considered a clean, renewable energy source. Thermal energy differs from heat energy in that energy is continuously exchanged between systems in contact even at thermal equilibrium. Within the crust, thermal energy is continuously transferred between the host rock and its formation fluids. According to the MIT panel (Tester et al., 2006), geothermal energy is generated either by (1) upward convection and conduction of heat from Earth's mantle and core, or (2) radioactive decay from elements in the crust, primarily from uranium, thorium, and potassium isotopes.

Specific subsurface conditions must exist within a geothermal reservoir before it is considered a feasible geothermal resource. First, the reservoir must exhibit relatively high heat flow and thermal gradient levels. Second, the particular depth of interest must be easily accessible and economically viable. Finally, the reservoir must have sufficient porosity and permeability to allow for circulation to effectively reheat the formation fluids via the high temperature host rock. It is

also recommended that the reservoir exhibit a relatively high recharge rate to ensure continuous production of the well. Enhanced Geothermal Systems (EGS) were created to extract economical amounts of heat from reservoirs that lack proper porosity and permeability by generating or enhancing interconnected fractures within the high temperature host rock. As reported by Tester et al. (2006), studies indicate that the most influential parameter affecting the amount of recoverable thermal energy is the fracture volume of the host rock. A large system of fractures allow for very slow moving fluids to achieve thermal equilibrium with the high temperature host rock.

Geothermal Power Plants. According to the Geothermal Energy Association (GEA) (2011), there are four types of geothermal power plants used to generate electricity: flash power, dry steam, binary, and flash/binary.

A flash power plant uses pressurized hot fluids at temperatures above 182°C (360°F). The fluids are separated by a steam separator (held at a lower pressure than the liquid) into steam and hot liquid. The steam is transported to a turbine to power a generator and the liquid is reinjected into the subsurface to be reused.

The most economically and environmentally favorable system is the dry steam power plant, where only available steam from the reservoir is used to power turbines and no separation of steam and liquid is necessary.

A binary power plant is useful for reservoirs with fluids at temperatures below approximately 150°C (300°F). The geothermal fluid that is extracted is used to heat a secondary fluid, with a boiling point below that of water. These liquids are kept separate using a heat exchanger that transfers heat from the geothermal fluid to the working fluid which expands into a gaseous vapor that drives the turbines. All extracted geothermal water is reinjected back into the reservoir through a closed-loop system.

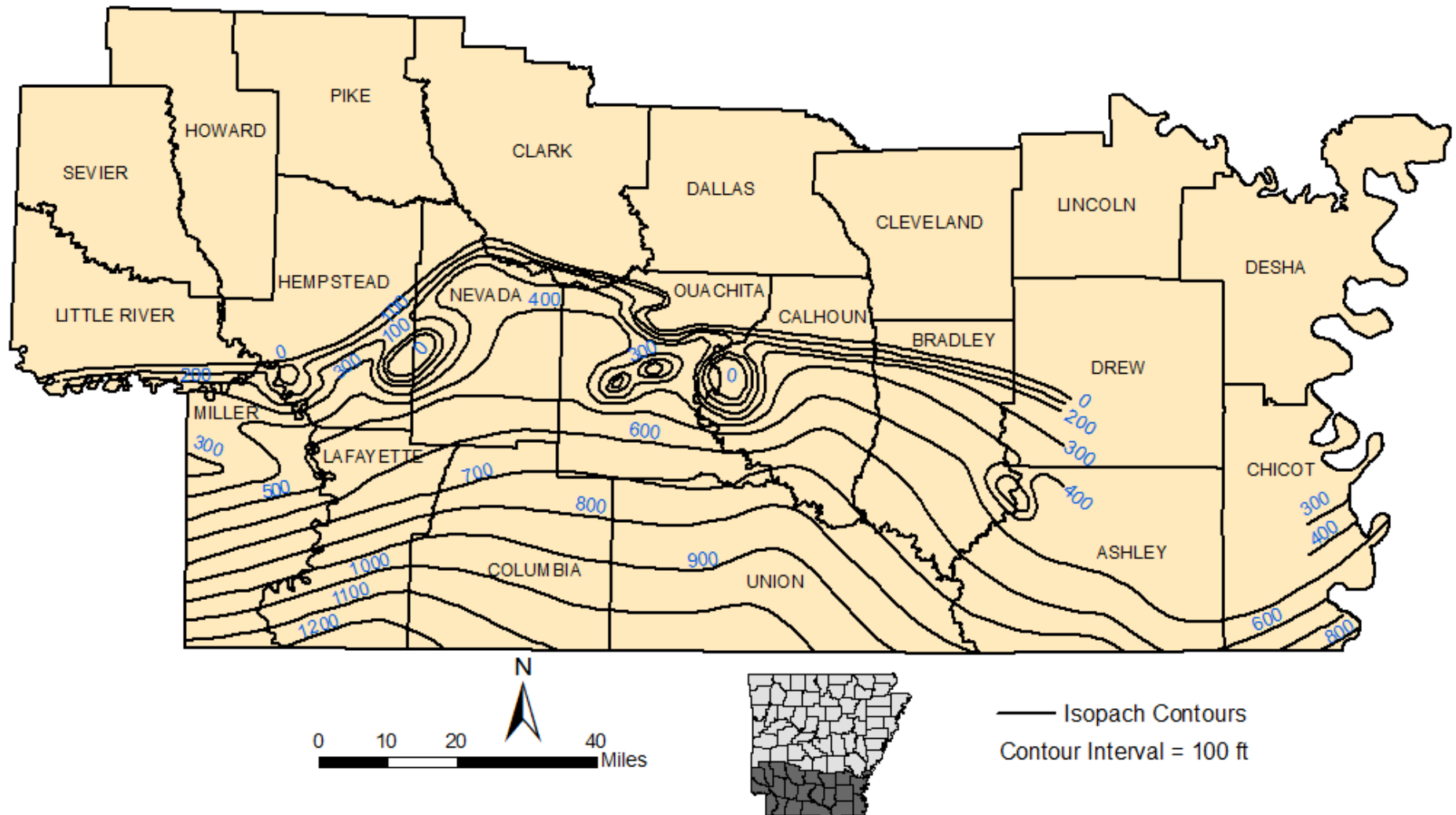


Figure 2. Isopach contours of top of Smackover Formation (modified from Vestal, 1950). Contour digitization by Jason Tipton, AGS.

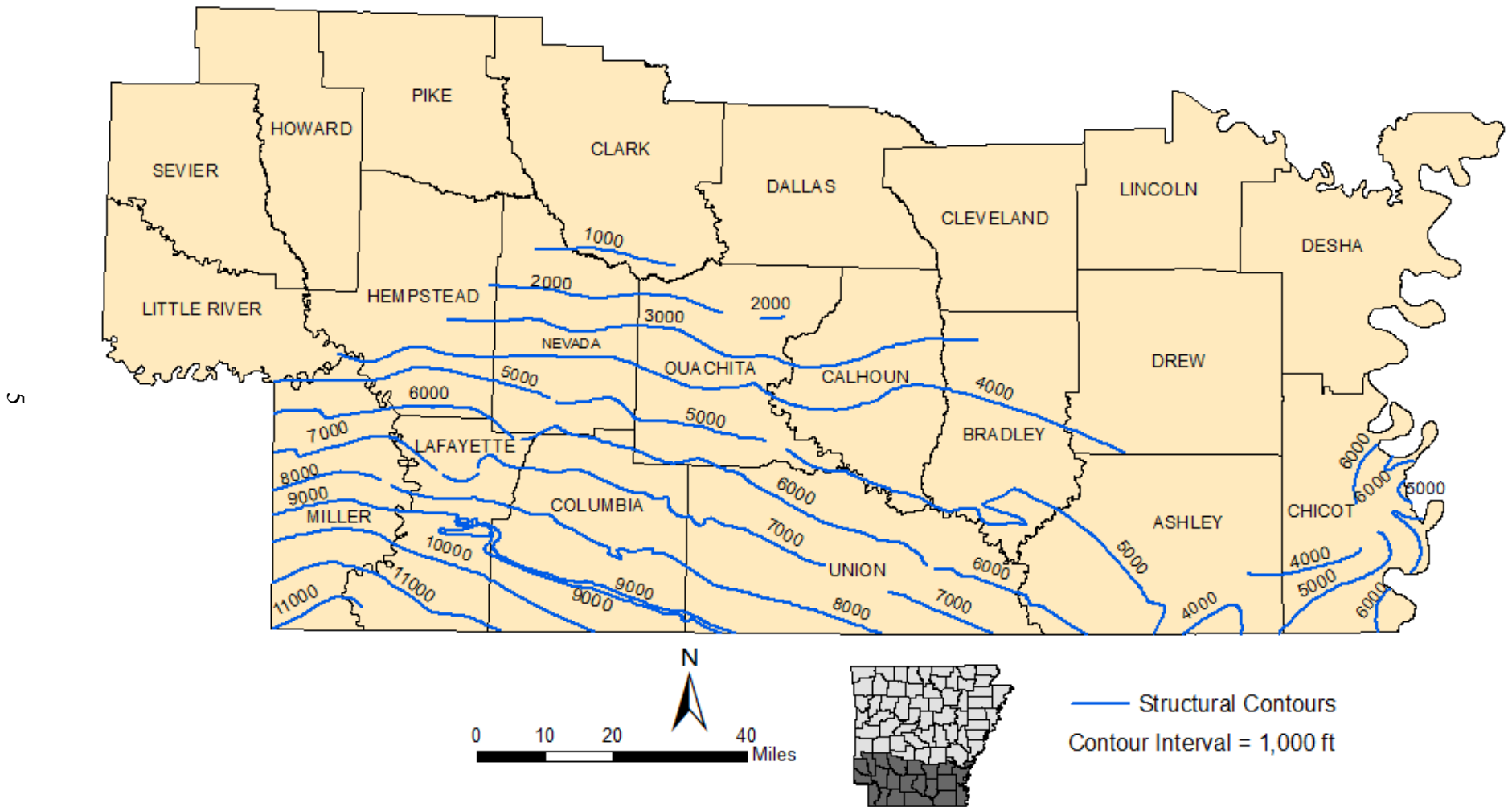


Figure 3. Structural contours of top of Smackover Formation (modified from Vestal, 1950). Contour digitization by Jason Tipton, AGS.

Since brines within the Smackover Formation in south Arkansas are at or near boiling, the binary system is the best choice for future Arkansas geothermal power plants.

Finally, the flash/binary combined cycle power plant uses both technologies. Like a flash system, the geothermal fluid that vaporizes into steam is under reduced pressure and directly turns the turbine while the steam exiting the turbine is condensed and used in a binary system.

Previous Smackover Geothermal Studies.

Numerous Smackover Formation electrical logs (circa 1930's to present) show recorded BHT's at or near boiling temperatures of water. A report on *Heat Flow Measurements in the State of Arkansas* (Roy et al., 1980) states that associated bromine-rich brines of the Smackover, extracted from depths of over 2,000 m (6,500 ft), are at temperatures near 100°C (212°F) upon reaching the surface. Recognizing the geothermal potential of these formation fluids, the Arkansas Power and Light, Co. (AP&L) (now part of Entergy Operations, Inc), in collaboration with the DOE, initiated a geothermal feasibility study near El Dorado, Arkansas in 1979. AP&L tested a 100kW direct contact boiling/condensing binary system using extracted brines from the Smackover to vaporize isopentane (C₅H₁₂), or the working fluid for this particular binary system, having a boiling point near 28°C (82°F) (Ellis, 1980). According to AP&L's plant manager, as reported by Ellis (1980), the plant operated intermittently from September through December 1979, during which several problems occurred as a result of control system issues, which allowed only short working intervals for the plant.

Possible Explanation of High Subsurface Temperatures in South Arkansas. Studies conducted by Southern Methodist University (SMU) Geothermal Laboratories indicate south Arkansas as having the warmest

subsurface temperatures, with the warmest of these areas along the Arkansas-Louisiana border. Although the origin of the warm brines in south Arkansas is not clearly understood, Smith and Dees (1982) suggest that the high heat flux in northern Louisiana may be attributed to abnormal concentrations of radiogenic heat sources within Cenozoic alkali igneous rocks of the Monroe Uplift, which extends from northeastern Louisiana into southeastern Arkansas.

Thermal Conductivity

Thermal conductivity is a measure of the ability of heat to flow through a particular material, and is a function of temperature. Thus, higher thermal conductivity values for a particular lithology indicate a higher allowance for heat flow. Thermal conductivity units for this project are measured in Watts per meter·Kelvin, (W/m·K). According to Clauser and Huenges (1995), the mineral content of a rock as well as its physical or diagenetic components will cause its thermal conductivity to vary by several factors. Porosity also influences thermal conductivity. The void spaces in high porosity rocks (>80%) are filled with low conducting air (0.024 W/m·K at 25°C) or water (0.58 W/m·K at 0°C).

Smackover Thermal Conductivity Sampling Method. A total of 131 core samples from 28 wells from southern Arkansas were measured for thermal conductance at the AGS owned Norman F. Williams Core Sample Library in Little Rock, Arkansas, and include units stratigraphically above and below the Smackover (Figure 4). Each well is assigned a permit number, a numeric identifier assigned to each drilled well in the state of Arkansas by the Arkansas Oil and Gas Commission (AOGC). Of the 131 measurements, 83 are Smackover core samples from 18 wells in southwest Arkansas; some samples include portions of the overlying Buckner Formation, typically a

red to gray shale. Thermal conductance results for the 10 non-Smackover wells are shown in Appendix 1.

Core samples selected for analyses were chosen based on (1) even distribution of well locations across southwest Arkansas, and (2) competency for drilling and thermal testing. However, thermal data were also collected on phonolite samples (permit number 21198) from the Monroe Uplift (potential origin of heat source) in Ashley County and are provided in Appendix 1.

Thermal measurements took place over a three month period beginning in mid-February 2012. All samples used in this project were from the AGS Norman F. Williams Core Sample Library. Thermal conductance was measured using a KD2 Pro Thermal Analyzer (version 1.08), purchased from Decagon Devices, Inc in 2011 (Figure 5). A Hilti Rotary Hammer was used to drill holes in the core using a 0.397 cm (5/32 in.) bit. Holes were drilled to the depth equal to the length of the thermal probe (Figure 6). After drilling was complete, compressed air removed debris from within the hole. The core was then set aside to cool to an average room temperature of 21°C (70°F) for at least ten minutes. After cooling, Arctic Alumina thermal grease (approximately 0.2 to 0.4 mL) was applied to the drilled hole. Thermal grease improves thermal contact between the thermal probe and the core; contact resistance will occur if no thermal grease is applied and will cause a decrease in normal thermal conductivity values registered by the probe. For better accuracy, measurements were set to run for ten minutes on High Power Mode (HPM). During the measuring process, the thermal probe increased in temperature for a length of time followed by a decrease, allowing the sensor in the probe to measure thermal properties of the sample.

A TR-1 thermal needle probe, with dimensions of approximately 9.9 cm (3.9 in.)

in length by 0.20 cm (0.10 in.) in diameter was originally provided with the analyzer specifically for core analysis. Several issues were noted when using the TR-1 probe on the core samples. First, drill bits equaling the dimensions of the probe were not readily available. Actual bits used for drilling were much wider than the diameter of the TR-1 probe, creating a significant gap between the core and probe. To account for this gap and allow for suitable thermal contact between the core and probe, a large amount of thermal grease (0.6 to 1 mL) was applied to the drilled hole. For some measurements, the amount of thermal grease added may have generated thermal results more reflective of the thermal grease (8 W/m·K, arcticsilver.com) and possibly contributed to higher error readings (≥ 0.02 or 2%). Also, the gap likely allowed more ambient air to come in contact with the probe, potentially lowering overall thermal conductance and increasing error values of the sample. Second, the probe requires 1 cm (0.40 in.) of rock surround the probe to allow the induced heat to be properly distributed throughout the sample. In most cases, samples of thermal interest did not meet this requirement and could not be measured. Finally, the diameters of most available core were approximately 8.9 cm (3.5 in.); therefore, no measurements parallel to bedding were recorded due to the probe length, thus eliminating the potential to determine lateral, or anisotropic, thermal characteristics, important in reservoir characterization for feasibility studies.

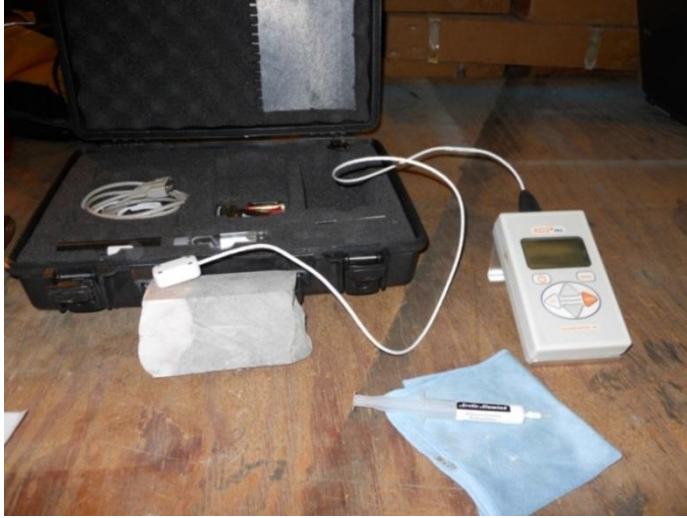


Figure 5. KD2 Pro Thermal Analyzer device showing probe inserted into core of interbedded anhydrite in dolostone. Thermal compound shown in tube in lower right.

Figure 6. Hilti rotary hammer used for core sample drilling.



To counter issues experienced with the TR-1 probe in thermal sampling, Decagon provided the AGS with a beta probe with dimensions of 6.4 cm (2.5 in.) long by 0.40 cm (5/32 in.) wide in early 2012. Drilling the appropriate beta probe dimensions within the core was simpler, which greatly increased the thermal contact between the core and probe, providing more reliable thermal measurements. Also, its shorter length allowed for measurements both perpendicular (isotropic) and parallel (anisotropic) to bedding. Overall, the beta

probe provided more consistent results among lithologies and generated lower error values compared to the TR-1 probe. Therefore, only the beta probe was used for further thermal measurements.

It is important to note that all five TR-1 measurements for three wells (permit numbers 21661, 26150, and 25774) are included in thermal conductivity and heat flow calculations (Table 1). However, all five measurements are in doubt due to measurement issues, high error values, and/or abnormally high or low thermal conductance

values, but are still considered relevant by providing the only available data for a specific lithology at a specific depth.

Thermal conductivity (W/m·K), thermal resistivity (°C·cm/W), error, initial temperature of the core sample (°C), sample ID (arbitrary), and read time (ten minutes per sample) data for each sample were uploaded from the device into Microsoft Excel (2010)[®].

According to the KD2 Pro Operator's Manual (2008-2010), error is a measure of how well the model resembles the data set, which is derived from algorithms generated from analyses of Carslaw and Jaeger (1959) and Kluitenberg et al. (1993). An optimal data set will provide errors lower than 0.01 (or 1%). For this project, note that the highest recorded error value of 0.26, measured by the TR-1 probe, was considered legitimate because comparable thermal conductance values were provided by similar lithologies with lower error values.

For each well, thermal conductance (λ_0) was measured at depths of lithologic interest (e.g. limestones, shales, and some sandstones). Lithologic descriptions of the Smackover Formation core samples, consisting primarily of oolitic grainstone to crystalline limestone, dolostone, and shale were also recorded (Table 1). Carbonates were described using the Dunham Classification System. Core sample photos of characteristic Smackover Formation are provided in Figures 7-9, with additional photos in Appendix 2. Thermal conductance results are provided for each well in map view in Figure 10 and listed in Table 1. For each core sample, a measurement was conducted either parallel or perpendicular (listed as para and perp in Table 1) to bedding for the possibility of determining horizontal and vertical components of heat flow in the

subsurface, respectively. However, as shown later in the thermal conductivity and heat flow maps, measurement orientation is not differentiated because thermal conductance values were similar in both directions. It appears measurement orientation had little effect; however, the orientation information may be important for future subsurface related studies in this area.

Thermal Conductance Correction for In Situ Conditions. Beardsmore and Cull (2001) state that thermal conductivity measured in a laboratory should be corrected for *in situ* temperature conditions. Sekiguchi (1984) provided an empirical correction equation that applies to any rock with a temperature range between 0-300°C (273-573 Kelvin (K)) (Equation 1).

$$\lambda = \left(\frac{T_0 T_m}{T_m - T_0}\right)(\lambda_0 - \lambda_m) \left(\frac{1}{T} - \frac{1}{T_m}\right) + \lambda_m \quad (1)$$

where

λ = corrected thermal conductivity

λ_m = 1.05 W/m·K, calibration coefficient

λ_0 = thermal conductivity at laboratory temperature, T_0

T_0 = temperature (K) at which λ_0 was measured (equal to the initial temperature of core sample recorded by the analyzer)

T_m = 1473 K (calibration coefficient)

Equation 1 was used to correct all AGS measured thermal conductance values (λ_{corr}) for *in situ* conditions. For each measurement, the corrected values were then averaged using the harmonic mean method to determine the average corrected thermal conductance (λ_{avg}) per well for the Smackover Formation (Table 1). The average corrected thermal conductance per well was then used to calculate average heat flow per well, described in the Heat Flow section.

Table 1. Smackover thermal conductance results showing measurement ID number, permit number of core, depth measured, thermal conductance, λ , (uncorrected, corrected, and average per well), error, measurement direction with respect to bedding (perp = perpendicular, para = parallel), and lithologic description of each sample. In order of increasing depth per well. TR-1 probe results in bold.

| ID # | Permit # | Depth (ft) | W/m·K | | | Err | Meas Dir | Lithologic Description |
|-----------|--------------|--------------|-------------|------------------|-----------------|-------------|--|---|
| | | | λ_o | λ_{corr} | λ_{avg} | | | |
| 5 | 21661 | 10810 | 4.04 | 2.97 | 1.79 | 0.02 | para | Fine-grained grainstone |
| 2 | 21661 | 10811 | 1.41 | 1.28 | | 0.07 | perp | Fine-grained grainstone |
| 3 | 21661 | 10812 | 2.38 | 1.44 | | 0.21 | perp | Fine-grained grainstone |
| 10 | 21661 | 10820 | 3.06 | 2.36 | | 0.02 | para | Anhydrite |
| 12 | 21661 | 10835 | 3.06 | 2.38 | | 0.01 | perp | Oolitic, pisolitic crystalline limestone |
| 11 | 21661 | 10836 | 3.68 | 2.77 | | 0.01 | para | Oolitic, pisolitic crystalline limestone |
| 13 | 26150 | 8545 | 3.76 | 3.01 | 2.47 | 0.01 | para | Fine-grained, shaley dolopackstone |
| 14 | 26150 | 8547 | 2.61 | 2.19 | | 0.01 | perp | Fine-grained, shaley dolopackstone |
| 15 | 26150 | 8549 | 2.40 | 2.03 | | 0.01 | para | Crystalline limestone |
| 16 | 26150 | 8551 | 3.85 | 3.10 | | 0.02 | perp | Oolitic, pisolitic crystalline limestone |
| 17 | 26150 | 8551.5 | 2.55 | 2.15 | | 0.01 | para | Oolitic, pisolitic crystalline limestone |
| 18 | 26150 | 8559 | 2.59 | 2.18 | | 0.03 | para | Oolitic, pisolitic crystalline limestone |
| 19 | 26150 | 8566 | 3.94 | 3.18 | 0.05 | para | Oolitic, pisolitic crystalline limestone | |
| 24 | 25774 | 9400 | 2.33 | 1.93 | 2.31 | 0.01 | perp | Red shale |
| 23 | 25774 | 9402 | 3.42 | 2.69 | | 0.01 | para | Crystalline dolostone |
| 25 | 25774 | 9403 | 5.48 | 4.05 | | 0.26 | perp | Fine-grained grainstone |
| 26 | 25774 | 9406 | 3.60 | 2.78 | | 0.01 | para | Fine-grained grainstone |
| 27 | 25774 | 9410 | 1.27 | 1.20 | | 0.09 | perp | Oolitic, pisolitic crystalline limestone |
| 28 | 25774 | 9411 | 2.53 | 2.06 | | 0.00 | perp | Oolitic, pisolitic crystalline limestone |
| 29 | 25774 | 9416 | 5.10 | 3.80 | | 0.12 | para | Oolitic, pisolitic grainstone |
| 30 | 25774 | 9425 | 3.18 | 2.51 | | 0.03 | perp | Oolitic, pisolitic grainstone |
| 31 | 25774 | 9430 | 2.91 | 2.33 | | 0.01 | perp | Oolitic, pisolitic grainstone |
| 32 | 27575 | 5299 | 2.24 | 2.01 | 1.73 | 0.01 | para | Oolitic, pisolitic grainstone |
| 33 | 27575 | 5302 | 2.61 | 2.32 | | 0.01 | para | Fine-grained, grainstone |
| 38 | 27575 | 5305 | 1.46 | 1.39 | | 0.01 | para | Fine-grained, grainstone; oomoldic ϕ |
| 35 | 27575 | 5310 | 1.94 | 1.77 | | 0.01 | para | Fine-grained oolitic, grainstone; oomoldic ϕ |
| 36 | 27575 | 5321 | 1.18 | 1.16 | | 0.01 | para | Fine-grained oolitic, grainstone; oomoldic ϕ |
| 37 | 27575 | 5322 | 2.10 | 1.90 | | 0.02 | perp | Fine-grained, dolograinstone; oomoldic ϕ |
| 39 | 27575 | 5339 | 2.54 | 2.26 | | 0.01 | para | Fine-grained grainstone |
| 40 | 27575 | 5349 | 1.85 | 1.70 | | 0.01 | para | Crystalline limestone |

Table 1 continued.

| ID # | Permit # | Depth (ft) | W/m·K | | | Err | Meas Dir | Lithologic Description |
|------|----------|------------|-------------|------------------|-----------------|------|----------|--|
| | | | λ_o | λ_{corr} | λ_{avg} | | | |
| 42 | 28603 | 9141 | 1.90 | 1.65 | 1.90 | 0.01 | perp | Dense, very fine-grained mudstone |
| 43 | 28603 | 9145 | 2.57 | 2.14 | | 0.01 | perp | Dense, very fine-grained mudstone |
| 41 | 28603 | 9148 | 2.66 | 2.20 | | 0.01 | perp | Dense, very fine-grained mudstone |
| 45 | 28603 | 9171 | 2.38 | 2.00 | | 0.00 | perp | Dense, very fine-grained mudstone |
| 44 | 28603 | 9174 | 1.68 | 1.50 | | 0.01 | perp | Dense, very fine-grained mudstone |
| 46 | 28603 | 9195 | 2.61 | 2.16 | | 0.02 | perp | Dense, very fine-grained mudstone |
| 59 | 18345 | 6328 | 1.82 | 1.67 | 1.69 | 0.01 | para | Possible lithic arenite |
| 60 | 18345 | 6334 | 1.40 | 1.33 | | 0.01 | para | Oolitic dolostone |
| 61 | 18345 | 6401 | 1.36 | 1.30 | | 0.01 | para | Fine-grained grainstone |
| 62 | 18345 | 6423 | 2.25 | 2.00 | | 0.01 | para | Fine-grained grainstone with organics |
| 63 | 18345 | 6425 | 2.22 | 1.98 | | 0.01 | para | Vugular crystalline limestone |
| 64 | 18345 | 6489 | 2.73 | 2.40 | | 0.01 | para | Vugular crystalline limestone with bitumen |
| 74 | 28258 | 6108 | 4.00 | 3.37 | 1.81 | 0.01 | para | Crystalline dolostone |
| 75 | 28258 | 6119 | 1.85 | 1.68 | | 0.02 | para | Oolitic grainstone |
| 76 | 28258 | 6125 | 1.39 | 1.32 | | 0.01 | para | Oolitic grainstone; oomoldic ϕ |
| 77 | 24087 | 5770 | 1.46 | 1.39 | 1.37 | 0.01 | perp | Oolitic grainstone; oomoldic ϕ |
| 78 | 24087 | 5782 | 1.43 | 1.37 | | 0.00 | perp | Oolitic grainstone; oomoldic ϕ |
| 79 | 24087 | 5868 | 1.25 | 1.22 | | 0.01 | perp | Fine-grained grainstone |
| 80 | 24087 | 5952 | 1.63 | 1.53 | | 0.00 | perp | Very fine-grained grainstone |
| 81 | 24227 | 7933 | 2.58 | 2.30 | 2.17 | 0.02 | perp | Oolitic, crystalline limestone |
| 82 | 24227 | 7950 | 2.05 | 1.86 | | 0.01 | para | Oolitic, fine-grained grainstone |
| 83 | 24227 | 7958 | 2.78 | 2.45 | | 0.00 | para | Fine-grained grainstone with organics |
| 88 | 26424 | 4277 | 4.12 | 3.63 | 2.47 | 0.01 | perp | Shaley dolowackestone to dolomudstone |
| 89 | 26424 | 4279 | 3.16 | 2.84 | | 0.01 | para | Fine-grained grainstone |
| 90 | 26424 | 4292 | 1.82 | 1.70 | | 0.00 | para | Oolitic, fine-grained grainstone |
| 109 | 30929 | 11095 | 3.726 | 2.86 | 2.28 | 0.00 | para | Fine-grained dolograinstone |
| 110 | 30929 | 11119 | 2.407 | 1.97 | | 0.01 | para | Oolitic, pisolitic crystalline limestone |
| 111 | 30929 | 11130 | 2.708 | 2.18 | | 0.01 | para | Oolitic, dense, crystalline limestone |
| 91 | 26489 | 7770 | 2.88 | 2.45 | 1.86 | 0.01 | para | Oolitic grainstone |
| 92 | 26489 | 7789 | 1.93 | 1.72 | | 0.01 | para | Oolitic, pisolitic grainstone |
| 93 | 26489 | 7846 | 1.86 | 1.68 | | 0.03 | perp | Oolitic, pisolitic crystalline limestone |
| 104 | 26677 | 5470 | 3.36 | 2.91 | 1.55 | 0.02 | para | Fine-grained dolograinstone |
| 105 | 26677 | 5472 | 1.06 | 1.05 | | 0.01 | perp | Fine-grained grainstone |
| 106 | 28301 | 5763 | 5.07 | 4.23 | 2.18 | 0.01 | perp | Red shale |
| 107 | 28301 | 5794 | 3.37 | 2.88 | | 0.01 | perp | Gray shale |
| 108 | 28301 | 5808 | 1.32 | 1.26 | | 0.01 | para | Oolitic grainstone |

Table 1 continued.

| ID # | Permit # | Depth (ft) | W/m·K | | | Err | Meas. Dir. | Lithologic Description |
|------|----------|------------|-------------|------------------|-----------------|------|------------|---|
| | | | λ_o | λ_{corr} | λ_{avg} | | | |
| 112 | 21807 | 10686 | 2.562 | 2.07 | 2.47 | 0.02 | perp | Fine-grained dolograinstone |
| 113 | 21807 | 10697 | 3.079 | 2.43 | | 0.01 | para | Crystalline limestone |
| 114 | 21807 | 10700 | 3.084 | 2.42 | | 0.00 | para | Crystalline limestone, small amt of anhydrite |
| 115 | 21807 | 10791 | 4.282 | 3.23 | | 0.02 | perp | Wackestone to mudstone |
| 116 | 28591 | 8217 | 3.928 | 3.18 | 2.57 | 0.01 | para | Crystalline limestone, small amt of anhydrite |
| 117 | 28591 | 8222 | 3.035 | 2.52 | | 0.00 | para | Fine-grained dolograinstone; oomoldic ϕ |
| 118 | 28591 | 8243 | 3.503 | 2.88 | | 0.02 | para | Oolitic, pisolitic fine-grained grainstone |
| 119 | 28591 | 8329 | 2.935 | 2.45 | | 0.01 | para | Fine-grained grainstone; oomoldic ϕ |
| 120 | 28591 | 8441 | 2.435 | 2.08 | | 0.01 | para | Fine-grained grainstone; oomoldic ϕ |
| 121 | 29667 | 8028 | 1.872 | 1.66 | 1.58 | 0.02 | para | Fine-grained, oolitic grainstone |
| 122 | 29667 | 8218 | 1.485 | 1.37 | | 0.01 | para | Fine-grained grainstone; oomoldic ϕ |
| 123 | 29667 | 8528 | 1.654 | 1.50 | | 0.01 | para | Dense, very fine-grained mudstone |
| 124 | 29667 | 8531 | 2.179 | 1.89 | | 0.01 | perp | Dense, very fine-grained mudstone |
| 125 | 29766 | 8603 | 2.329 | 2.00 | 1.86 | 0.00 | para | Oolitic grainstone |
| 126 | 29766 | 8621 | 2.113 | 1.84 | | 0.01 | para | Fine-grained, oolitic grainstone |
| 127 | 29766 | 8654 | 2.471 | 2.10 | | 0.01 | para | Fine-grained grainstone |
| 128 | 29766 | 8727.5 | 1.784 | 1.59 | | 0.01 | para | Fine-grained grainstone |



Figure 7. Oolitic grainstone of the upper Smackover Formation. Permit number 26489, western Union County. Core diameter is 8.9 cm (3.5 in.).



Figure 8. Oolitic to pisolitic crystalline limestone of the upper Smackover Formation. Permit number 30929, southwestern Columbia County.



Figure 9. Oolitic grainstone exhibiting oomoldic porosity. Permit number 28301, southeastern Nevada County. Sample length approximately 20 cm (8 in). Probe hole in center of core.

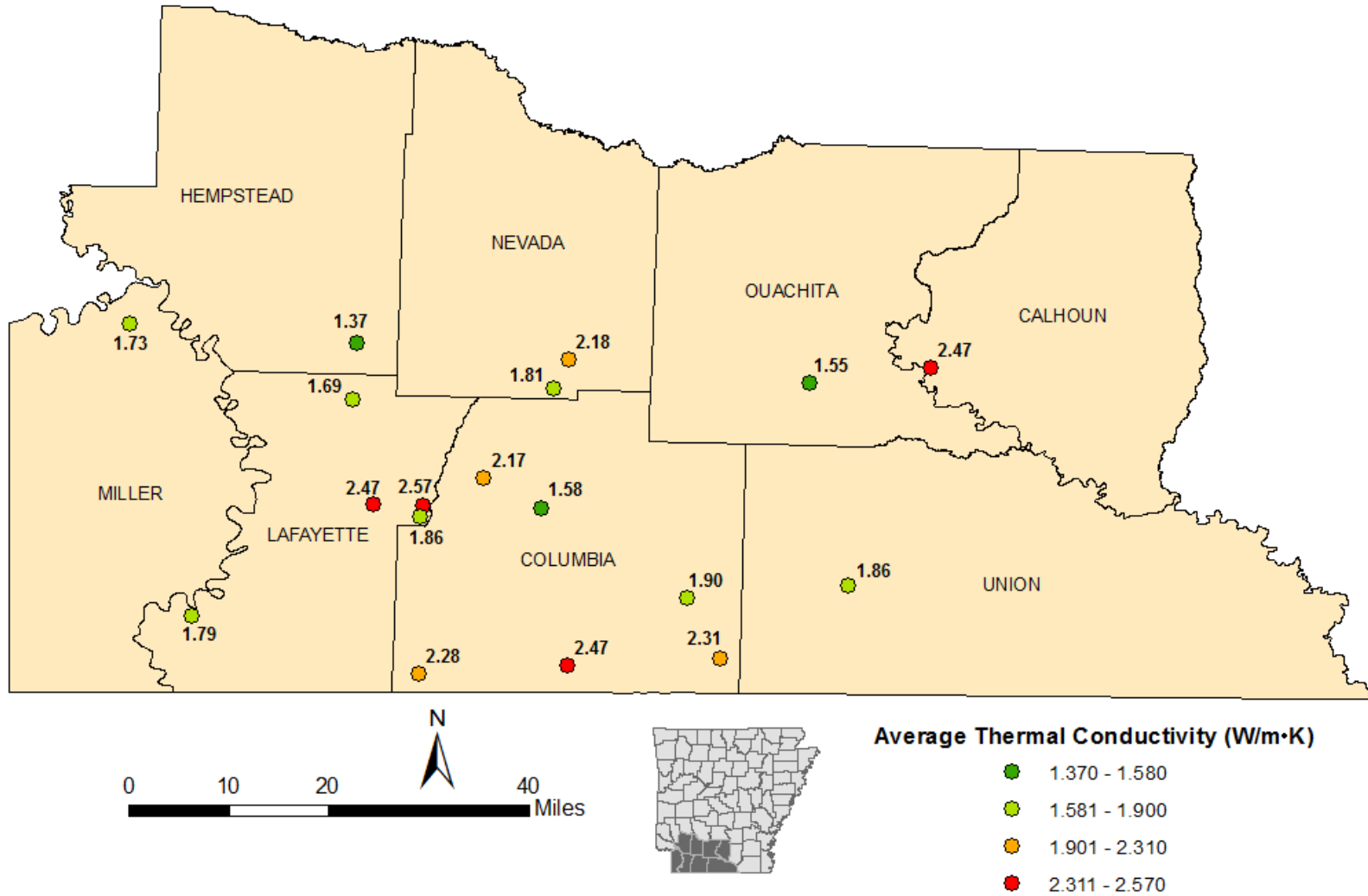


Figure 10. Average thermal conductance values for each Smackover well in W/m·K.

Thermal Conductance Results. The highest estimated average thermal conductance value for a Smackover well is 2.57 W/m·K for a fine-grained grainstone, permit number 28591, located in eastern Lafayette County (Figure 10). The next highest average thermal conductance values are for permit numbers 26424 (Calhoun County), 21807 (Columbia County), and 26150 (eastern Lafayette County) all measuring 2.47 W/m·K with lithologies consisting of fine-grained grainstone and crystalline limestone. The highest single, corrected thermal conductivity value for a Smackover well is 4.23 W/m·K for a red shale (lowermost Buckner, uppermost Smackover), permit number 28301 in southern Nevada County. These results indicate an area of higher relative thermal conductance for the Smackover Formation in northeastern Lafayette County and southern Nevada County.

To validate the reliability of the range of values generated by the KD2 Pro Thermal Analyzer, published thermal conductivities (W/m·K) for shale, limestone, mudstone, dolostone, and anhydrite were compared with thermal conductivities of all 83 core samples of the Smackover Formation measured at the AGS (Table 2). Average thermal conductance values for each measured lithology were calculated using harmonic mean. All grainstone and crystalline limestone were categorized as limestone; wackestone, mudstone, dolowackestone, and dolomudstone were classified as mudstone; and all dolograins and dolopackstone were classified as dolostone.

Average AGS thermal conductance values for shale, limestone, mudstone, and dolostone lie within the range of at least one published value; however, the single sampled anhydrite value is less than the published

value. This discrepancy may be reduced if more anhydrite samples are measured and averaged and more comparison data is available to validate these results.

Thermal Gradient

According to Beardsmore and Cull (2001), thermal gradient is defined as a vector that is dependent on temperature distributed in three dimensions (x , y , and z axes). Knowing three-dimensional temperature distributions within the crust is ideal for determining the true vector of the maximum thermal gradient, but three dimensional data is rarely available for calculations. To account for this deficiency, it is assumed that maximum thermal gradient is vertical within the upper crust with the Earth's surface forming a horizontal, constant temperature boundary. This minimizes lateral temperature variation at depth. This assumption permits thermal gradient to reduce to one vertical dimension (Equation 2)

$$\Delta T = \frac{\partial T}{\partial z} \mathbf{k} \quad (2)$$

where ΔT is the temperature distribution function, gradient $(\frac{\partial T}{\partial z})$ is the derivative of temperature with respect to depth, and \mathbf{k} is the vector along the vertical axis (z axis).

To calculate a basic geothermal gradient, temperatures at two or more depths must be known. The more temperature to depth ratios available, the more accurate the gradient values. Borehole temperatures and temperature logs provide temperature to depth data and are the best available resources for calculating geothermal gradients.

Table 2. Comparing published thermal conductance values (W/m·K) with AGS thermal conductance values for varying lithologies.

| Lithology | Beardsmore (1996) * | Majorowicz & Jessop (1981) * | Beach et al. (1987) * | Reiter & Jessop (1985) * | Reiter & Tovar (1982) + | AGS Average n = 83 # |
|------------------|---------------------|------------------------------|-----------------------|--------------------------|-------------------------|----------------------|
| Shale | 2.9 | 1.5 ± 0.5 | 1.4 ± 0.4 | 2.1 ± 0.4 | 2.1 ± 0.4 | 2.7 |
| Limestone | 3.1 | 2.9 ± 0.9 | 2.4 ± 0.9 | 2.8 ± 0.4 | 2.8 ± 0.3 | 1.9 |
| Mudstone | 2.9 | -- | -- | -- | 2.0 ± 0.4 | 2.0 |
| Dolostone | -- | 5.0 ± 0.6 | 3.1 ± 1.4 | 4.7 ± 0.8 | 4.7 ± 1.1 | 2.3 |
| Anhydrite | -- | -- | -- | -- | 5.4 ± 0.4 | 2.4 |

* Indicates published compilations of thermal conductivities reported from Beardsmore and Cull (2001).

+ Indicates published thermal conductivity reported from Reiter and Tovar (1982) averaged from Clark (1966) and Reiter (1969).

Indicates AGS average based on harmonic mean.

Correcting for In Situ Borehole Temperatures Using the Harrison Correction Equation. During the well drilling process, drilling fluid is injected and circulated through the well to cool the drill bit. The presence of cool fluid affects thermal equilibrium of the formation and borehole conditions at the base of the well where fluid collects. Upon completion of drilling, logging devices measure certain parameters of the borehole, including BHT. These BHT measurements are unreliable estimates of *in situ* temperatures because of the induced unequilibrated conditions. The amount of time required for the formation to reach thermal equilibrium depends on certain factors, such as drilling conditions, drilling mud temperature at the surface, circulation rate, and thermal conductivity of the surrounding formation (Harrison et al., 1983). According to Beardsmore and Cull (2001), drilling fluids typically reach equilibrium at approximately ten times the total drilling time.

To approximate *in situ* temperature conditions within the well, Harrison et al. (1983) developed the Harrison Correction Equation (Equation 3) derived from a correction curve representing the deviation of BHT's from true formation temperature.

$$\text{Meters: } T_c = -2.3449E-006 * x^2 + 0.01826842109x - 16.51213476 \quad (3)$$

where T_c is the corrected temperature subtracted or added to the original BHT values and x is the depth in meters. For wells deeper than 3,900 m (12,800 ft), the correction is a constant increase of 19.1; for wells below 1,220 m (4,000 ft), the correction is negative and is subtracted from the BHT; and under 600 m (2,000 ft), no correction is used.

The Harrison Equation was used to correct all BHT's from the Smackover Formation in southwest Arkansas (Table 3).

The resulting corrected temperature, T_c , was applied to BHT's to generate a temperature value more representative of *in situ* formation fluids and surrounding rock conditions of the Smackover (Corrected Temp °C).

Determining Estimated Geothermal Gradients for Southwest Arkansas. After calculating corrected temperatures, geothermal gradient values were determined for the 18 Smackover wells. In some instances, multiple runs occurred where several BHT's at varying depth intervals were recorded. To calculate an overall geothermal gradient ($\frac{\Delta T}{\Delta Z}$) for wells with multiple runs, the difference in consecutive BHT's were averaged generating an overall geothermal gradient for the well. In most cases, only one run was conducted for each well where the geothermal gradient was calculated by comparing the temperature at depth to the average surface temperature. Roy et al. (1980) reports that compiled information from weather stations in Arkansas's Gulf Coastal Plain show an average surface temperature of 17.2°C (63.1°F). Table 3 shows Harrison Correction calculations and results along with average geothermal gradient per well in °C/100 m and Kelvin/m (K/m); Kelvin units are necessary for heat flow calculations discussed later. The average geothermal gradients per well from Table 3 were plotted in ArcMap and shown in Figure 11. In conjunction, a raster image was created from the point data using the nearest neighbor method in Spatial Analyst ArcGIS 10.1 and is illustrated in Figure 12. Harrison Correction, corrected temperatures, and geothermal gradient values for the 10 non-Smackover wells are provided in Appendix 3.

Corrected Geothermal Gradient Results and Comparison. Observation of corrected Smackover geothermal gradient values

shows that the highest gradients fall between 3.36°C/100m (1.8°F/100 ft) and 3.46°C/100m (1.9°F/100 ft) in western Calhoun County, southern Columbia County, and southern Nevada County (Figure 11). A comparison of thermal conductivity and thermal gradient values as well as a thermal

gradient heat map (Figure 12) show that southern Columbia County, southern Nevada County, and western Calhoun County have the greatest geothermal potential. However, additional heat flow values are needed to further establish these areas as having the greatest geothermal potential.

Table 3. Harrison correction (Equation 3), corrected temperature, and estimated average geothermal gradient values for 18 Smackover wells in southwest Arkansas.

| Permit # | Total Depth (m) | MaxTemp (°C) from well log | Harrison Correction (T _c) | Corrected Temp °C | Geothermal Gradient °C/100m | Geothermal Gradient K/m (for determining heat flow) | Heat Flow mW/m ² (refer to heat flow section below) |
|----------------------|-----------------|----------------------------|---------------------------------------|-------------------|-----------------------------|---|--|
| 21661 | 3343 | 107 | 18.35 | 125.35 | 3.24 | 0.0324 | 58.1 |
| 26150 | 2632 | 80 | 15.33 | 95.33 | 2.97 | 0.0298 | 73.4 |
| 25774 | 2972 | 100 | 17.07 | 117.07 | 3.36 | 0.0337 | 77.6 |
| 27575 | 1699 | 64.4 | 7.75 | 72.20 | 3.24 | 0.0325 | 56.1 |
| 28603 | 2889 | 90 | 16.69 | 106.69 | 3.10 | 0.0310 | 59.0 |
| 18345 | 1981 | 68.89 | 10.47 | 79.36 | 3.14 | 0.0315 | 53.3 |
| 28258 | 1983 | 73.89 | 10.49 | 84.38 | 3.39 | 0.0340 | 61.7 |
| 24087 | 1755 | 60 | 8.33 | 68.33 | 2.91 | 0.0292 | 40.0 |
| 24227 | 2419 | 79.44 | 13.96 | 93.40 | 3.15 | 0.0315 | 68.4 |
| 26677 | 1758 | 66.67 | 8.35 | 75.02 | 3.29 | 0.0330 | 51.1 |
| 28301 | 1934 | 71.11 | 10.04 | 81.16 | 3.31 | 0.0332 | 72.4 |
| 30929 | 3414 | 105 | 18.52 | 123.52 | 3.11 | 0.0312 | 71.2 |
| 21807 | 3303 | 110 | 18.25 | 128.25 | 3.36 | 0.0337 | 83.3 |
| 28591 | 2591 | 85 | 15.08 | 100.08 | 3.20 | 0.0321 | 82.4 |
| 29667 | 2609 | 87.78 | 15.19 | 102.96 | 3.29 | 0.0330 | 52.2 |
| 29766 | 2731 | 87.78 | 15.89 | 103.67 | 3.17 | 0.0317 | 59.0 |
| 26489 | 2438 | 77.78 | 14.09 | 91.87 | 3.06 | 0.0307 | 58.1 |
| 26424 | 1372 | 60.56 | 4.13 | 64.69 | 3.46 | 0.0348 | 85.8 |
| Harmonic mean | | | | | 3.20 | 0.0321 | 62.2 |

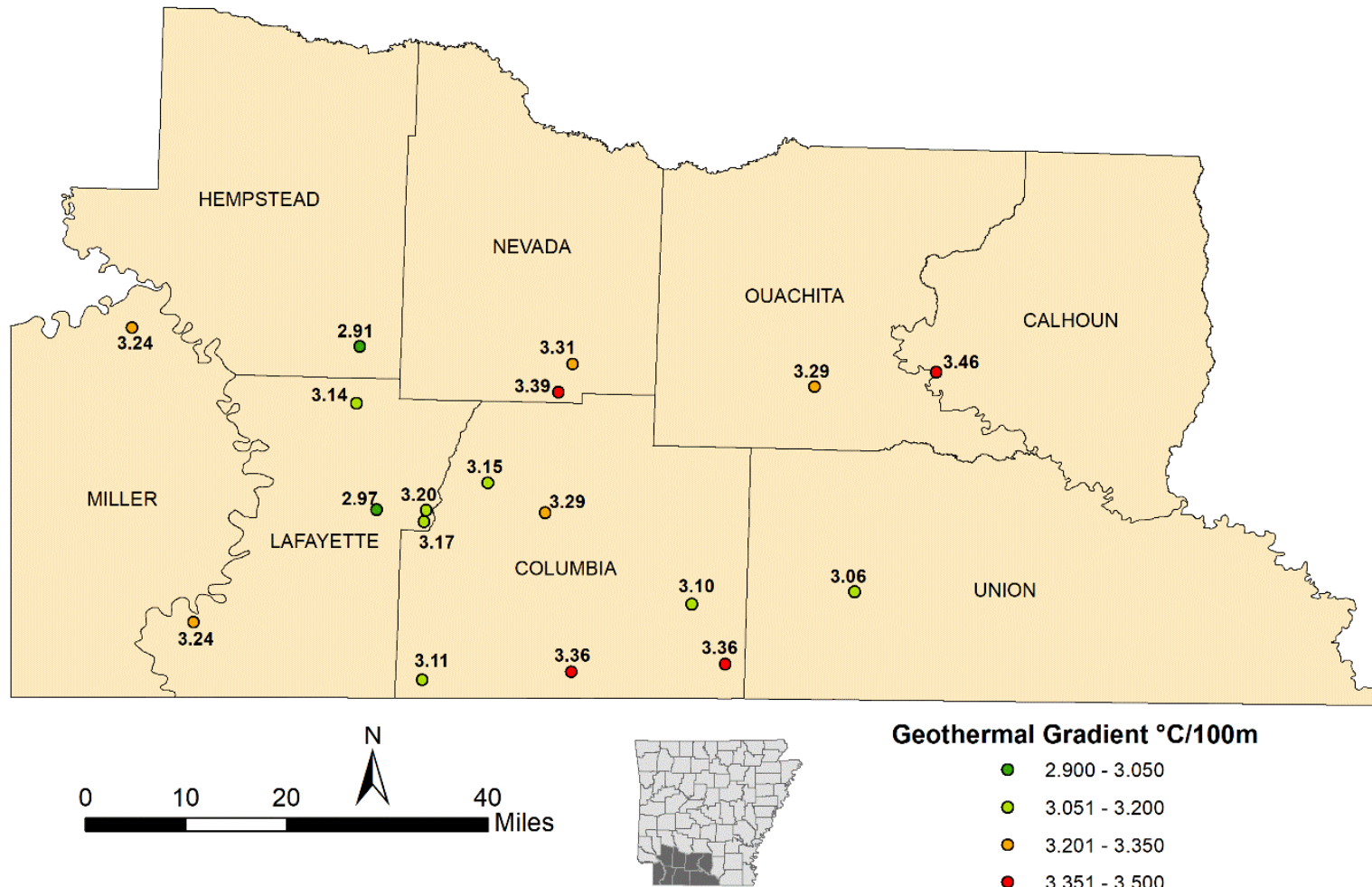


Figure 11. Geothermal gradient values for each Smackover well in °C/100m.

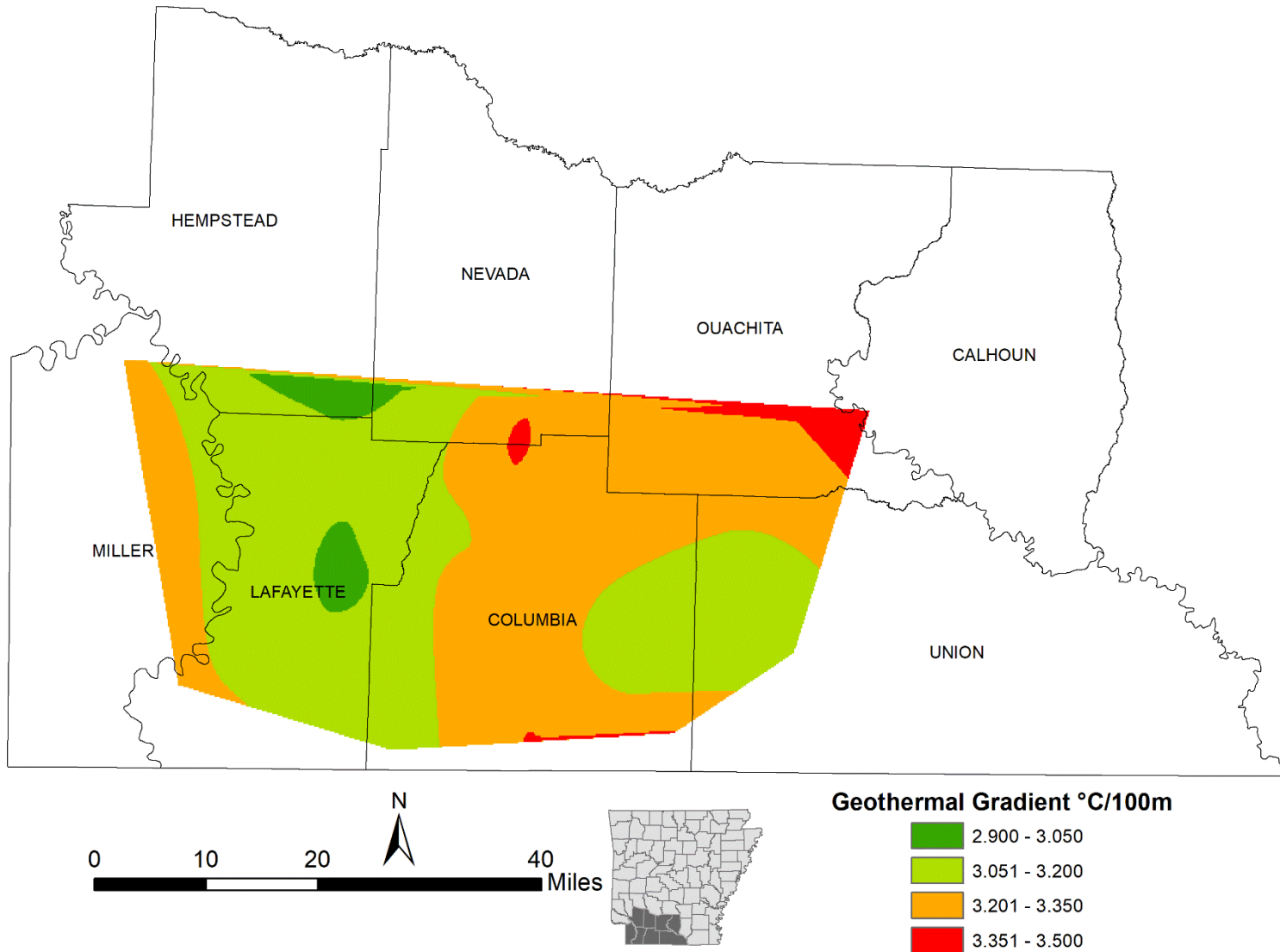


Figure 12. Geothermal gradient heat map of the Smackover Formation in °C/100m. Generated using the natural neighbor method in Spatial Analyst in ArcGIS.

Heat Flow

Heat flow is the transfer of thermal energy from one body to another or a transfer of temperature. As aforementioned, heat within the crust is generated by either radioactive decay, primarily from uranium, thorium, and potassium, or through conduction and convection from the Earth's interior. The conveyance of heat through the crust is primarily related to rock type and structure (Smith and Fishkin, 1988).

Calculating Geothermal Heat Flow. Heat flow (Q) is the product of the harmonic average thermal conductivity (λ_{avg}) and the harmonic average geothermal gradient ($\frac{\partial T}{\partial z}$) (Equation 4).

$$Q = \lambda_{avg} \times \left(\frac{\partial T}{\partial z}\right)_{avg} \quad (4)$$

Heat Flow, in units of milliwatts per meter per meter (mW/m^2), was determined for the 18 Smackover wells using calculated geothermal gradients from the last column in Table 3 (K/m) and harmonic mean thermal conductivity (λ_{avg}) from Table 1 ($W/m \cdot K$) (last column, Table 3).

Discussion of Estimated Heat Flow Maps. Three heat flow maps (Figures 13-15) were generated for the 18 wells of the Smackover Formation in southwest Arkansas. Figure 13 shows the estimated heat flow values per well. A raster heat flow map (Figure 14) was generated from the heat flow values in Figure 13 using the natural neighbor method in Spatial Analyst, ArcGIS. Heat flow contours were generated from the raster image and are shown in Figure 15.

The harmonic average heat flow for the 18 Smackover wells is $62.2 mW/m^2$. For rate comparison, an MIT panel (Tester et al., 2006) reports geothermal heat flows through

the Earth's crust at an average rate of $59 mW/m^2$. A previous heat flow investigation in Arkansas (Smith and Fishkin, 1988) indicated a heat flow value of $68 mW/m^2$ located near the town of Jerome in Drew County, southeast Arkansas.

Figure 13 shows a well in western Calhoun County having the highest estimated heat flow value near $86 mW/m^2$ (permit number 26424). Figures 14 and 15 show the areas of highest heat flow exist on the northern and southeastern boundaries of the study area in southern Nevada, western Calhoun, and southern Columbia Counties. An additional high exists in eastern Lafayette County. The last column of Appendix 3 lists the estimated heat flow data for the 10 non-Smackover wells.

Heat flow values for most of southwest Arkansas range from 51 to $75 mW/m^2$ and are lowest in southeast Hempstead County ($40 mW/m^2$) (Figure 13). An updated geothermal heat flow map of the conterminous U.S. produced by SMU's Geothermal Laboratory in 2011 shows heat flow values for southwest Arkansas ranging from approximately 60 to $100 mW/m^2$ (Blackwell et al., 2011). Figure 16 shows heat flow data for southern Arkansas sourced from the global heat flow database of the International Heat Flow Commission in 2010. This map shows that the highest heat flow for southwest Arkansas is in northwest Miller County ($\sim 90-100 mW/m^2$), which is located farther west of the highest heat flow values projected by the AGS (Figures 14 and 16). However, Figure 16 also exhibits a few spots of increased heat flow in southeast Nevada County and western Calhoun County, which are consistent with the AGS's data.

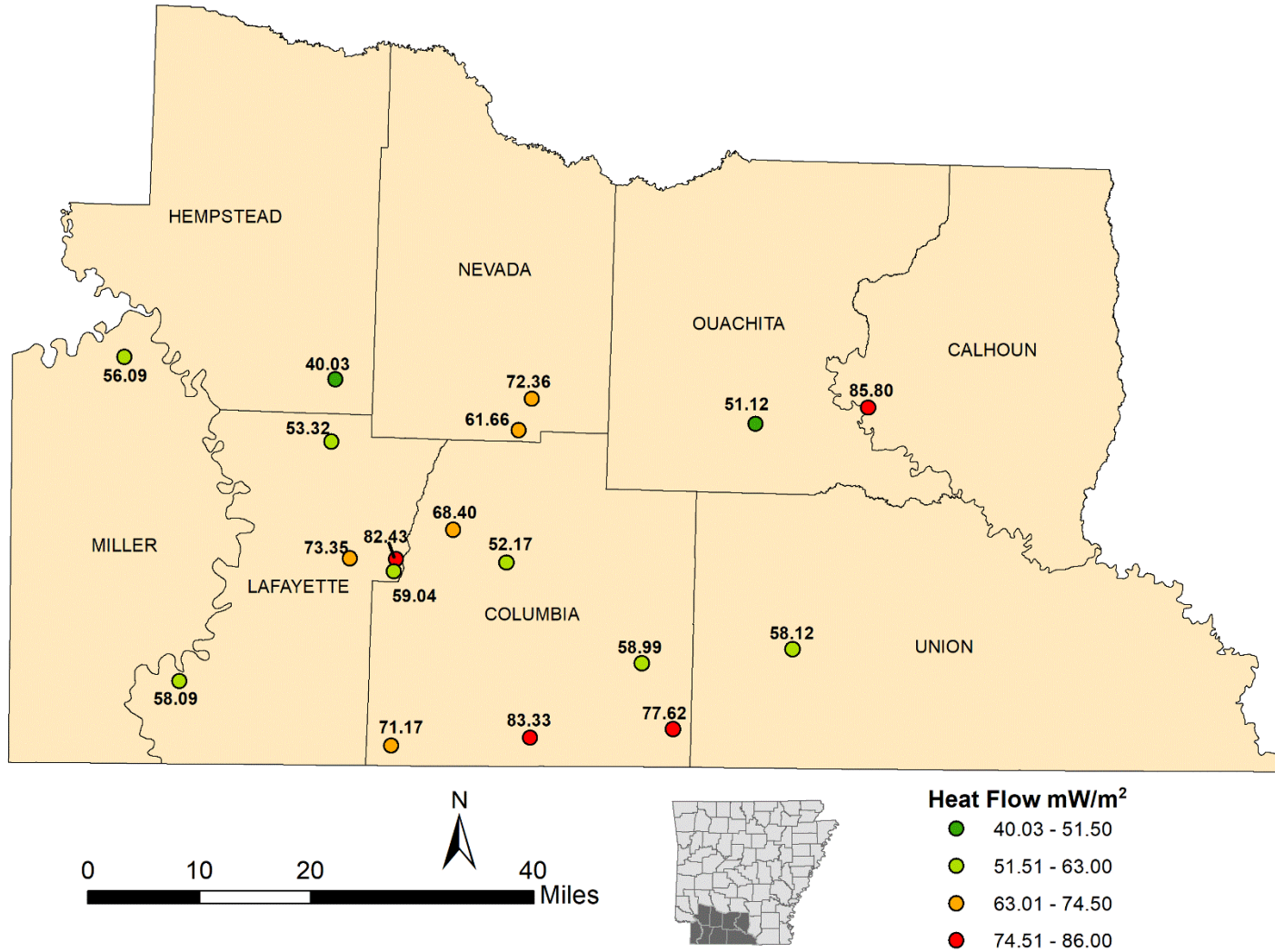


Figure 13. Estimated heat flow for each Smackover Formation well in mW/m^2 . The harmonic mean heat flow value is approximately 62 mW/m^2 . Labeled according to actual heat flow values.

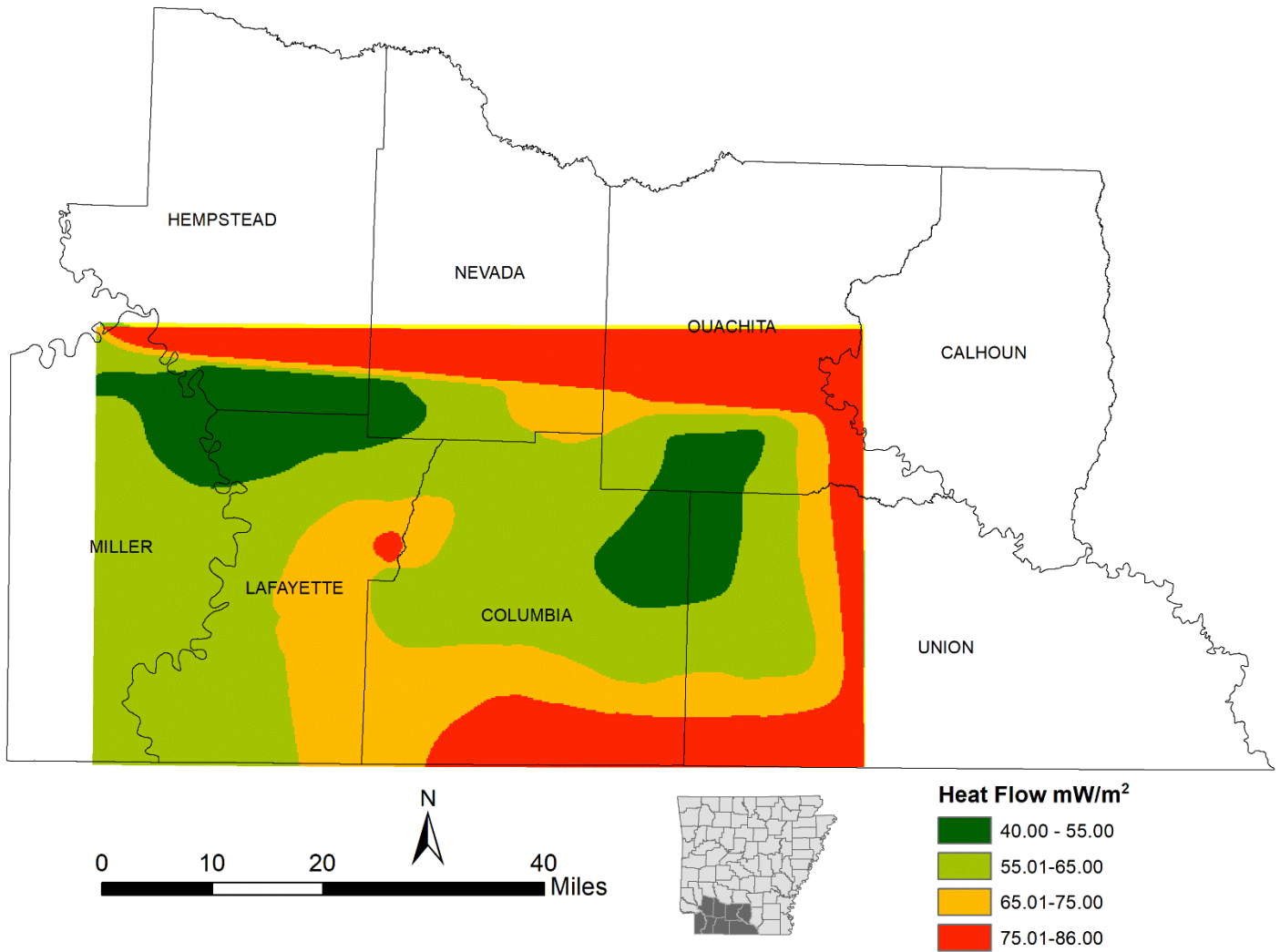


Figure 14. Estimated heat flow map of southwestern Arkansas. Generated using the natural neighbor method in Spatial Analyst in ArcGIS.

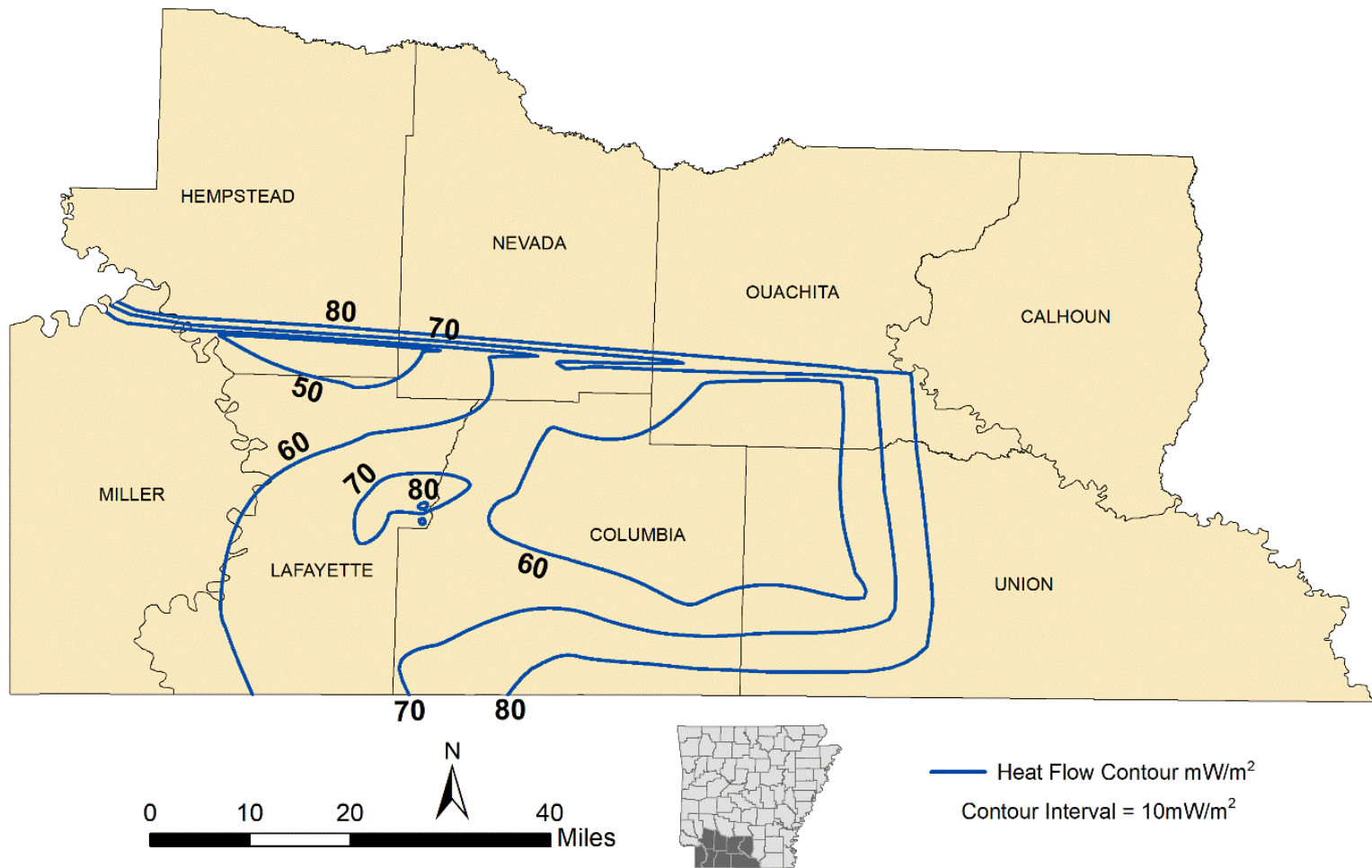


Figure 15. Estimated heat flow contour map of the Smackover Formation.

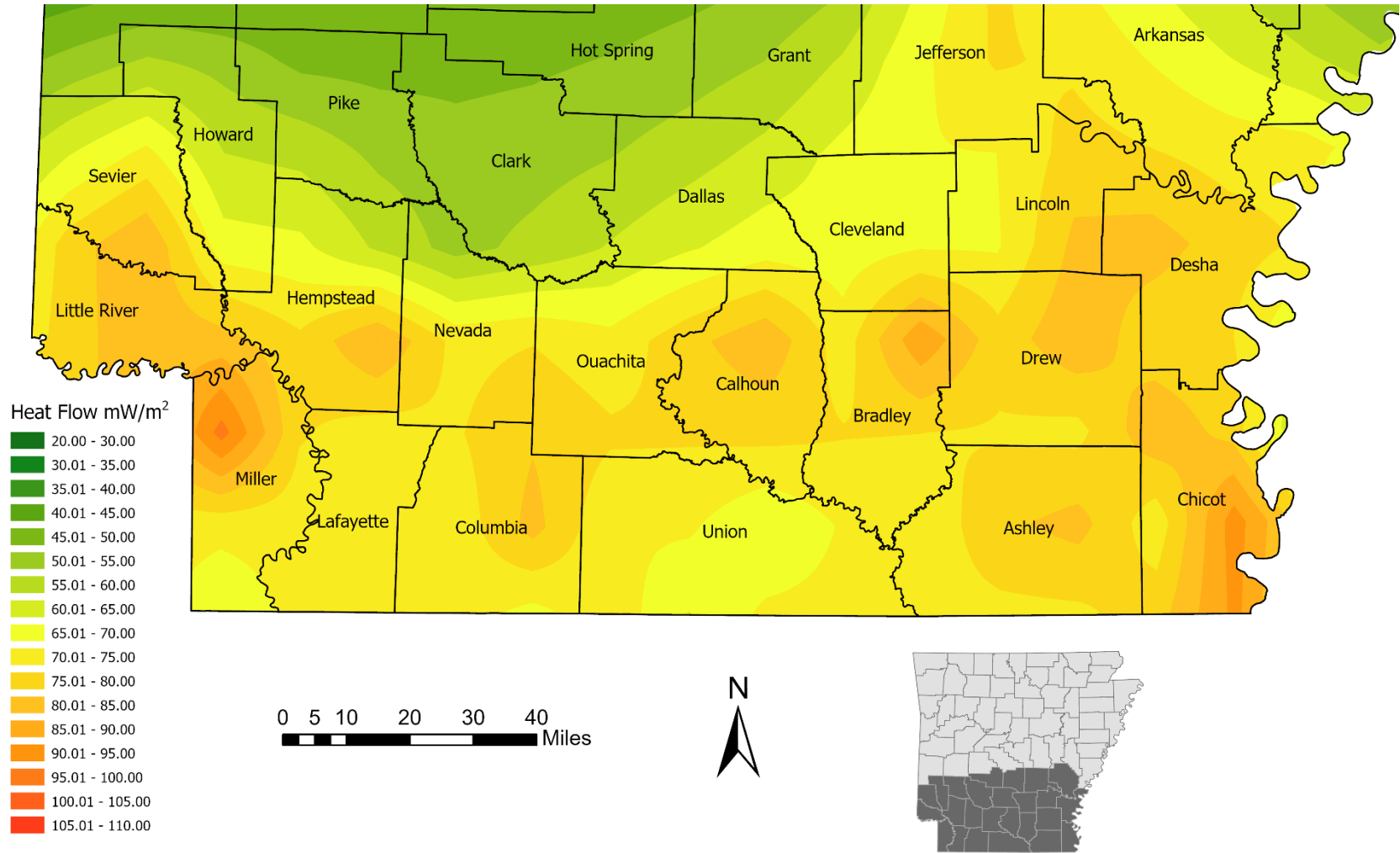


Figure 16. Heat flow data for southern Arkansas sourced from the global heat flow database of the International Heat Flow Commission (2010).

Verification of Data

Near the conclusion of this publication, two Smackover samples, permit numbers 21661 (southwest Lafayette County) and 25774 (southeast Columbia County), were sent to the University of North Dakota (UND), Harold Hamm School of Geology and Geological Engineering Laboratory for thermal conductance testing. This was at the request of the State Geothermal Data team to verify thermal conductance results measured by the AGS. The samples were chosen by an AGS staff member for the geothermal project and not for this publication. However, the laboratory results provide the only exclusive verification of the thermal conductivity data measured at the AGS, thus it is important to discuss this information briefly.

The UND samples were measured using a Portable Electronic Divided Bar (PEDB), a device that uses an upper and lower brass plate to measure thermal conductivity under *in situ* conditions. For these samples, thermal conductance was measured through an isolated system with heat flow running vertically and maintained at a constant temperature of 20°C (68°F). Samples were cut into small pieces and polished to create smooth flat surfaces for proper contact with the plates. Conductivity values were calibrated using polycarbonate disks. Each sample was measured twice and averaged.

For permit number 21661, the measured depth interval was 3,304 m (10,839 ft) for an oolitic to pisolitic, crystalline limestone. For permit number 25774, the depth interval was 2,878 m (9,441 ft) for a fine-grained grainstone. These intervals are higher than the intervals measured at the AGS; therefore, the UND results were considered to be average thermal conductivities for each well and were

compared to the AGS average thermal conductivity values for the corresponding well, λ_{avg} (Table 1).

UND results for permit numbers 21661 and 25774 are 2.91 and 2.47 W/m·K, respectively (the device manufacturer claims an accuracy of $\pm 3.5\%$). These values are higher than the corrected values calculated at the AGS. However, as shown in Table 1, both wells include TR-1 probe measurements. As aforementioned, TR-1 results are questionable due to measurement issues related to the dimensions of the probe but are still considered relevant by providing the only available data for a specific lithology at a specific depth. After removing the TR-1 results from these two wells, leaving only the beta probe results, the average thermal conductance for permit number 21661 was 2.59 W/m·K, and for permit number 25774 was 2.48 W/m·K, values much closer to the UND results.

Using these recalculated averages, heat flow values increase to around 84 mW/m² for both wells. A new heat flow map and contour map were produced with this change and results are presented in Figures 17 and 18, respectively. The most dramatic difference between these figures and Figures 14 and 15 is that higher heat flow values from 65 – 86 mW/m² extend westward into Lafayette and Miller County.

All in all, the UND results are similar to the corrected results measured by the beta probe, verifying that the AGS results are accurate estimations of *in situ* thermal conductivity of the Smackover Formation.

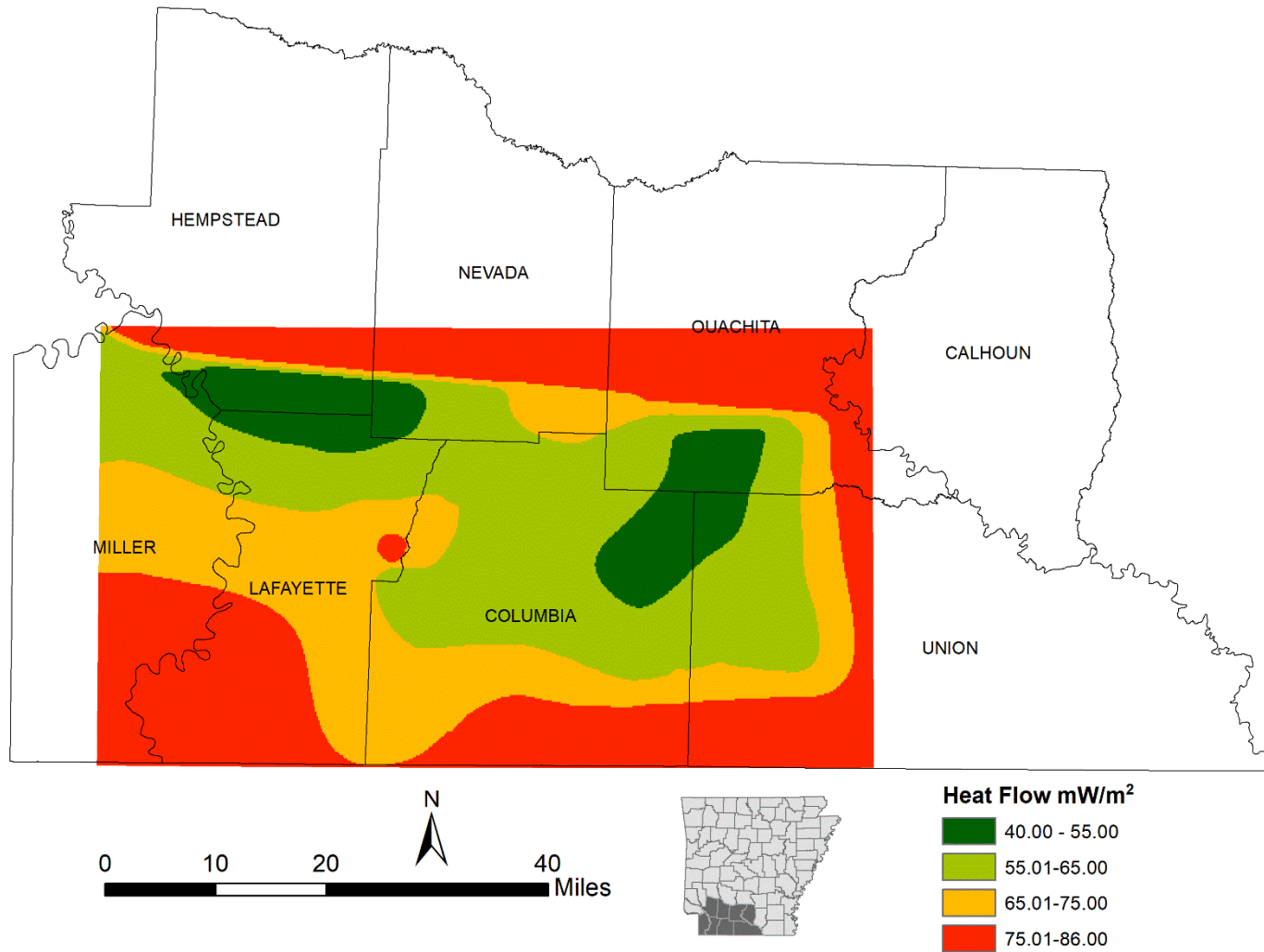


Figure 17. Estimated heat flow map of southwestern Arkansas with recalculated average heat flows (84 mW/m²) for permit number 21661 (southwest Lafayette County) and permit number 25774 (southeast Columbia County).

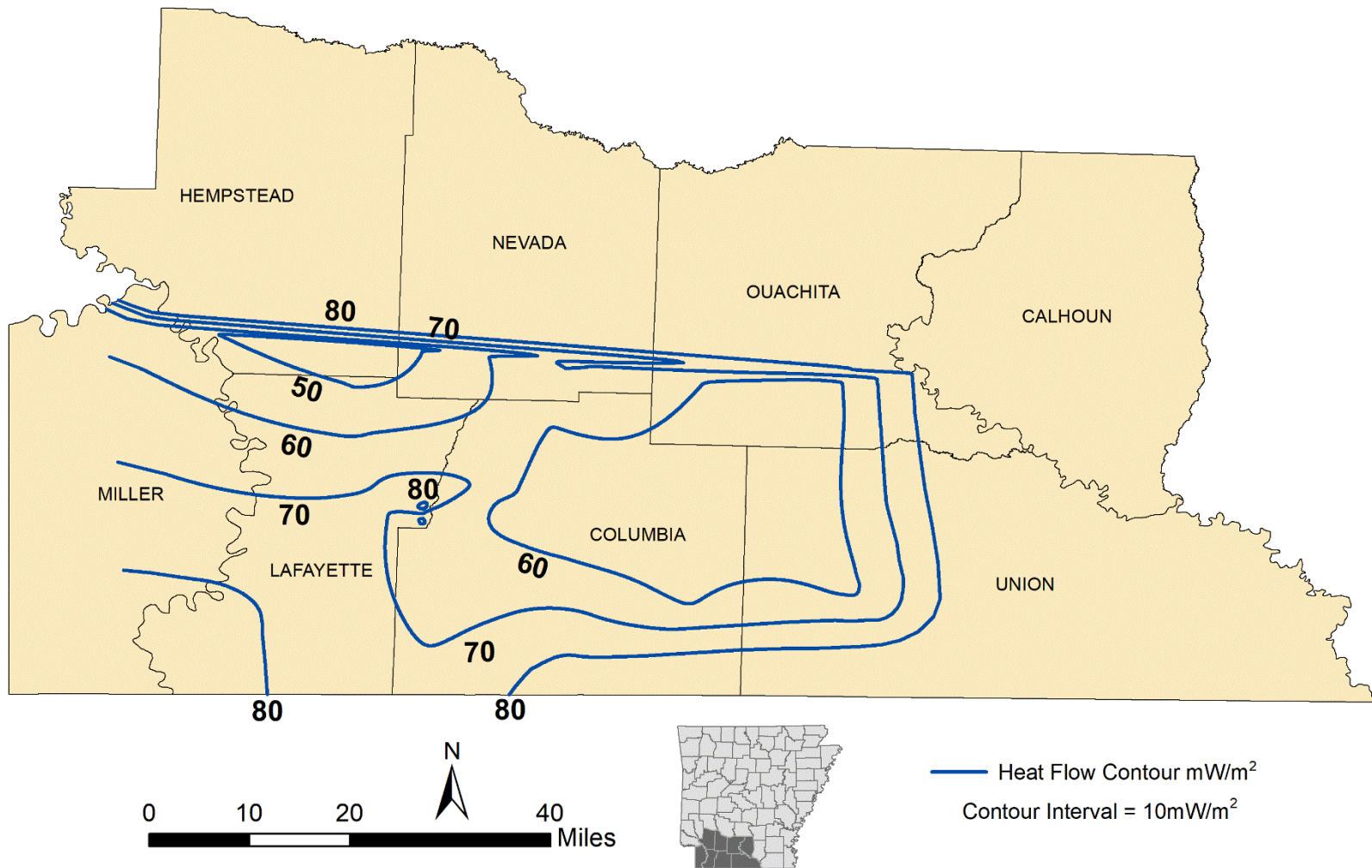


Figure 18. Estimated heat flow contour map of the Smackover Formation with recalculated average heat flows (84 mW/m²) for permit number 21661 (southwest Lafayette County) and permit number 25774 (southeast Columbia County).

Conclusion

Based on the collected data for the Smackover Formation, southern Columbia, southern Nevada, and western Calhoun Counties show the highest geothermal potential. These areas exhibit geothermal gradients and heat flow values that are slightly higher than the average values for continental crust at 25°C/km and 65 mW/m², respectively (Criss, 2019).

Thermal gradient, thermal conductance, and heat flow values are estimations of the Smackover Formation. Thermal conductance estimations were verified through comparison with thermal conductance values measured at UND and through comparison with available published data.

Some observed borehole temperatures for the Smackover Formation across south Arkansas are near boiling. If using the Smackover Formation as a geothermal resource for industrial purposes, the binary geothermal power plant is the most feasible option. The binary power plant utilizes formation fluid temperatures near or below boiling to heat a secondary fluid which operates a turbine to generate electricity. In south Arkansas, a binary power plant operated intermittently in mid-1979, but was quickly shut down due to operating issues.

New borehole technology is capable of determining more accurate *in situ* BHT's and thermal conductance values. Therefore, further investigations characterizing the Smackover Formation's *in situ* BHT's and thermal properties are recommended for future geothermal feasibility studies of southwest Arkansas.

References

- Arctic Silver Thermal Compound. Accessed 2012. <<http://www.arcticsilver.com>>
- Arkansas Geological Survey Subsurface Stratigraphic Chart. Accessed 2012. <http://geology.ar.gov/energy/oil_productionarea.htm>
- Beach, R.D., F.W. Jones, and J.A. Majorowicz, 1987. Heat Flow and Heat Generation Estimates for the Churchill Basement of the Western Canadian Basin in Alberta, Canada. *Geothermics*, Vol. 16, Issue 1, p. 1-16.
- Beardsmore, G.R., 1996. The Thermal History of the Browse Basin and its Implications for Petroleum Exploration. Ph.D. dissertation, Monash University, Victoria, Australia. 238 p.
- Beardsmore, G.R. and J.P. Cull, 2001. Crustal Heat Flow. A Guide to Measurement and Modelling. Cambridge University Press, 319 p.
- Blackwell D.D. and M. Richards, 2004b. Calibration of the AAPG Geothermal Survey of North America BHT Data Base. AAPG Annual Meeting, Dallas, TX. Poster session, paper 87616. <<http://smu.edu/geothermal/bht/aapg04%20blackwell%20and%20richards.pdf>>
- Blackwell, D.D., Richards, M.C., Frone, Z.S., Batir, J.F., Ruzo, A.A., and Dingwall, R.K., 2011. SMU Geothermal Laboratory Heat Flow Map of the Conterminous United States, 2011. Supported by Google.org
- <https://www.smu.edu/-/media/Site/Dedman/Academics/Programs/Geothermal-Lab/Graphics/SMUHeatFlowMap2011_CopyrightVA0001377160_jpg.jpg>
- Carslaw, H.S. and J.C. Jaeger, 1959. Conduction of Heat in Solids. Second Edition. Oxford, London. 517 p.
- Clark, S.P., 1966. Thermal Conductivity, in Clark, S.P., Jr., ed., Handbook of Physical Constants: Geol Soc Am Mem. 97, p. 459-482.
- Clauser, C. and E. Huenges. 1995. Thermal Conductivity of Rocks and Minerals in Ahrens, T.J. ed., Rock Physics and Phase Relations: A Handbook of Physical Constants: American Geophysical Union Shelf 3, p. 105-126.
- Criss, R.E., 2020. Thermal models of the continental lithosphere, in Hofmeister, A.M., ed., Heat Transport and Energetics of the Earth and Rocky Planets: Elsevier, p. 151-174.
- Ellis, P.F. II, 1980. Geothermal Materials Survey Arkansas Power and Light Development and Demonstration Project. 100 kW Power System Using Direct Contact Heat Exchangers, El Dorado, Arkansas. U.S. Department of Energy. 27 p. <<http://www.osti.gov/bridge/servlets/purl/5034780-oSQu7F/native/5034780.pdf>>
- Geothermal Energy Association, Accessed 2011, May 26. <<http://geo-energy.org/Basics.aspx>>

- Global Heat Flow Database, 2010. KMZ file download. Accessed February, 2023. <<https://www.datapages.com/gis-map-publishing-program/gis-open-files/global-framework/global-heat-flow-database>>
- Harrison, W.E., K.V. Luza, M.L Prater, and P.K Cheung, 1983. Geothermal Resource Assessment in Oklahoma. Special Publications 83-1. Oklahoma Geological Survey. <http://www.ogs.ou.edu/pubsscanned/SPs/SP83_1.pdf>
- Kluitenberg, G.J., J.M Ham, and K.L Bristow, 1993. Error Analysis of the Heat Pulse Method for Measuring Soil Volumetric Heat Capacity. *Soil Sci. Soc. Am. J.* 57: p. 1444-1451.
- Majorowicz, J.A. and A.M. Jessop, 1981. Regional Heat Flow Patterns in the Western Canadian Sedimentary Basin. *Tectonophysics*. Vol. 74, Issue 3-4, p. 209-238.
- Ober, J.A (USGS). 2012. Industrial Minerals Review 2011. *Min Eng*. V. 64, No. 6, p. 40-41.
- Plebuch, R.O., 1962. Ground-water Temperatures in the Coastal Plain of Arkansas. USGS Water Resources Summary No. 2. 6 p.
- Reiter, M.A., 1969. Terrestrial Heat Flow and Thermal Conductivity in southwestern Virginia. Ph.D. thesis, Virginia Polytechnic Institute, Blackburg, Virginia. 103 p.
- Reiter, M.A. and R.J.C. Tovar, 1982. Estimates of Terrestrial Heat Flow in Northern Chihuahua, Mexico. *Geol Soc Am Bull*. Vol 93, No. 7, p. 613-624.
- Reiter, M.A. and A.M. Jessop, (1985). Estimates of Terrestrial Heat Flow in Offshore Eastern Canada. *Can J Earth Sci*, Vol. 22, Issue 10, p. 1503-1517.
- Roy, R.F., B. Taylor, A.J. Pyron, and J.C. Maxwell, 1980. Heat Flow Measurements in the State of Arkansas. Final report to the University of California, Los Alamos Scientific Laboratory. <<http://library.lanl.gov/cgi-bin/getfile?00311086.pdf>>
- Sekiguchi, K., 1984. A method for determining terrestrial heat flow in oil basinal areas. *Tectonophysics*, Vol. 103, Issue 1-4, p. 67-79.
- Smith D.L. and W.T. Dees. 1982. Heat Flow in the Gulf Coastal Plain. *J Geophys Res*. Abstract, V.87, No. B9.
- Smith, D.L. and L. Fishkin. 1988. New Heat Flow Investigations in Arkansas. Contributions to the Geology of Arkansas, Arkansas Geological Commission. Misc. Pub 18-C, V. III, p. 79-84.
- Tester, J.W., B.J. Anderson, A.S. Batchelor, D.D. Blackwell, R. DiPippo, E.M. Drake, J. Garnish, B. Livesay, M.D. Moore, K. Nichols, S. Petty, M. Nafi Toksöz, R.W. Veatch, Jr., R. Baria, C. Augustine, E. Murphy, P. Negraru, and M. Richards. 2006. The Future of Geothermal Energy. Impact of Enhanced Geothermal Systems (EGS) on the United States in the 21st Century. An assessment by an MIT-led interdisciplinary panel. Accessed July, 2012. <http://www1.eere.energy.gov/geothermal/egs_technology.html>

Vestal, J.H., 1950. Petroleum Geology of the Smackover Formation of Southern Arkansas. Information Circular 14, Arkansas Geological Commission. 37 p.

Weeks, W.B., 1938. South Arkansas Stratigraphy with Emphasis in the Older Coastal Plain Beds. *Am Assoc Pet Geol Bull*, Vol. 22, No. 8, p. 953-983.

Appendices

Appendix 1. Results of the 10 non-Smackover wells showing measurement ID number, permit number of core, depth measured, thermal conductance, λ (uncorrected, corrected, and average per well), error, measurement direction with respect to bedding (perp = perpendicular, para = parallel), and lithologic description of each sample.

| ID # | Permit # | Depth (ft) | W/m·K | | | Err | Meas Dir. | Unit | Lithologic Description |
|------|----------|------------|-------------|------------------|-----------------|------|-----------|------------|---|
| | | | λ_o | λ_{corr} | λ_{avg} | | | | |
| 47 | 25103 | 4912 | 1.43 | 1.37 | 1.51 | 0.01 | perp | Sligo | Oolitic, fine-grained grainstone |
| 48 | 25103 | 4915 | 1.54 | 1.47 | | 0.01 | para | | Oolitic, fine-grained grainstone |
| 49 | 25103 | 4917 | 1.61 | 1.53 | | 0.01 | para | | Oolitic, crystalline limestone |
| 50 | 25103 | 4930 | 1.83 | 1.70 | | 0.02 | para | | Fine-grained wackestone |
| 65 | 22027 | 2493 | 1.26 | 1.24 | 1.32 | 0.02 | perp | Tuscaloosa | Tan, fine-grained, quartz arenite |
| 66 | 22027 | 2525 | 1.16 | 1.15 | | 0.01 | para | | Tan, fine-grained, quartz arenite |
| 67 | 22027 | 2528 | 1.71 | 1.65 | | 0.01 | perp | | Tan, fine-grained, quartz arenite |
| 68 | 22549 | 2488 | 3.07 | 2.92 | 3.32 | 0.02 | para | Tuscaloosa | lt.- gray, v. fine-grained, quartz arenite, low porosity |
| 69 | 22549 | 2510 | 3.26 | 3.10 | | 0.01 | perp | | lt.- gray, v. fine-grained, quartz arenite, with 1" shale bed at top of sample, low to med porosity |
| 70 | 22549 | 2531 | 4.39 | 4.16 | | 0.00 | perp | | dk-brown to black, fine-grained quartz arenite, low porosity Org/petro residue on sample |
| 71 | 24755 | 2063 | 2.65 | 2.63 | 2.63 | 0.02 | perp | Nacatoch | Md.-gray, v fine-grained packestone to wackestone |
| 84 | 21198 | 3939 | 1.27 | 1.23 | 1.34 | 0.00 | para | Intrusion | Igneous Phonolite with pyrite |
| 85 | 21198 | 3943 | 1.56 | 1.46 | | 0.01 | para | | Igneous Phonolite with pyrite |
| 86 | 21198 | 5044 | 3.81 | 3.29 | 3.28 | 0.01 | para | Unknown | Dk- gray, crystalline limestone |
| 87 | 21198 | 5067 | 3.78 | 3.26 | | 0.02 | perp | | V. dk-gray to black, crystalline limestone |
| 94 | 27520 | 2130 | 3.80 | 3.71 | 2.86 | 0.06 | perp | Nacatoch | Dk.-gray. Fine-grained wackestone to mudstone. Org/petro residue on sample |
| 95 | 27520 | 2133 | 2.37 | 2.33 | | 0.01 | perp | | Md.-gray, fine-grained dolomitic wackestone to mudstone. |

Appendix 1 continued.

| ID # | Permit # | Depth (ft) | W/m K | | | Err | Meas. Dir. | Unit | Lithologic Description |
|------|----------|------------|-------------|------------------|-----------------|------|------------|---|---|
| | | | λ_o | λ_{corr} | λ_{avg} | | | | |
| 96 | 27370 | 4376 | 2.5 | 2.26 | 2.28 | 0.03 | para | Sligo | Lt.-gray, grainstone w/interbedded crystalline limestone |
| 97 | 27370 | 4376 | 2.1 | 1.94 | | 0.02 | para | | Sandstone, mudstone with flaser bedding. Jumbled zone |
| 98 | 27370 | 4384 | 2.7 | 2.43 | | 0.01 | perp | | Lt.-gray, fossiliferous grainstone, almost boundstone-like, high porosity |
| 99 | 27370 | 4399 | 3.4 | 3.06 | | 0.01 | para | | Brown fine-grained mudstone with shale interbeds, jumble zone |
| 100 | 27370 | 4405 | 2.2 | 2.03 | | 0.01 | para | | Shaley dolomudstone with flaser-like bedding |
| 101 | 20071 | 11282 | 2.36 | 1.92 | | 2.09 | 0.01 | | perp |
| 102 | 20071 | 11289 | 3.03 | 2.37 | 0.01 | | perp | Dk.-gray, dense, v. fine-grained crystalline limestone, little to no porosity | |
| 103 | 20071 | 11310 | 2.51 | 2.02 | 0.01 | | perp | Dk.-gray, dense, v. fine-grained crystalline limestone, little to no porosity | |
| 129 | 25837 | 3693 | 4.67 | 4.23 | 2.61 | 0.03 | perp | Tuscaloosa | Gray, fine-grained, friable quartz arenite with laminations of dk-gray shale |
| 130 | 25837 | 3701 | 2.00 | 1.89 | | 0.02 | para | | Gray, fine-grained, friable quartz arenite with coalified markings throughout |
| 131 | 23829 | 7489 | 2.06 | 1.76 | 1.76 | 0.01 | perp | Eagle Mills | Red, fine-grained crystalline limestone with fossil fragments |

Appendix 2. Additional photographs of Smackover Formation core samples.



1. Dolostone with anhydrite, likely part of the upper Smackover Formation or lower Buckner Formation. Permit number 28591, eastern Lafayette County. Hand lens for scale. Notice fingernail mark in anhydrite underlined in red.

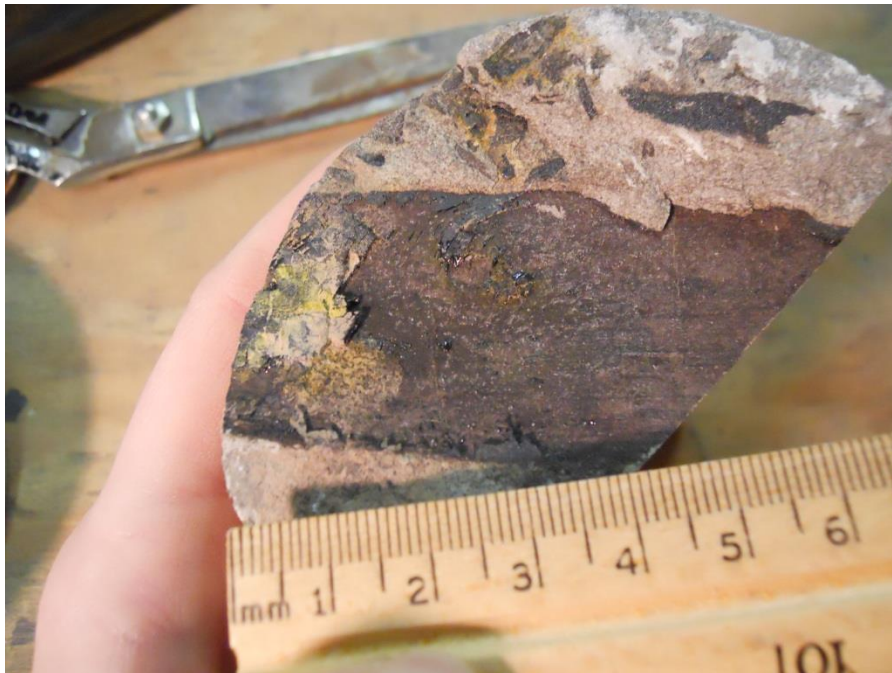


2. High amplitude stylolite filled with organics in upper Smackover Formation. Permit number 28591, eastern Lafayette County. Hand lens for scale.

Appendix 2 continued.



3. Possible allochems within crystalline limestone sample of upper Smackover Formation. Permit number 30929, southwestern Columbia County. Core diameter approximately 8.9 cm (3.5 in.). Hand lens for scale.



4. Coalified surface in fine-grained grainstone, upper Smackover Formation. Permit number 25774, southeastern Columbia County. Ruler for scale.

Appendix 3. Harrison Correction, corrected temperatures, and geothermal gradient values for 10 non-Smackover wells in south Arkansas.

| Permit # | Location | Total Depth (m) | MaxTemp (°C) from well log | Harrison Correction (T _c) | Corrected Temp °C | Geothermal Gradient °C/100m | Geothermal Gradient K/m (for determining heat flow) | Heat Flow (mW/m ²) |
|---------------------------------------|---------------------------|-----------------|----------------------------|---------------------------------------|-------------------|-----------------------------|---|--------------------------------|
| 25103 | Western Miller Co | 1515 | 54.4 | 5.78 | 60.2 | 2.84 | 0.0285 | 43.0 |
| 22027 | Northern Lafayette Co | 793 | 48.9 | -3.49 | 45.4 | 3.55 | 0.0358 | 47.2 |
| 22549 | Northern Lafayette Co | 734 | 44.4 | -4.36 | 40.1 | 3.12 | 0.0314 | 104.2 |
| 24755 | Eastern Ouachita Co | 671 | 34.4 | -5.31 | 29.1 | 1.78 | 0.0180 | 47.6 |
| Run 1: 21198 (phonolite) | Northeastern Ashley Co | 1717 | 68.3 | 7.94 | 76.3 | 3.44 | 0.0345 | 46.2 |
| Run 2: 21198 (limestone) | | | | | | | | 113.1 |
| 27520 | Central Union Co | 710 | 37.8 | -4.72 | 33.1 | 2.23 | 0.0226 | 64.7 |
| 27370 | Southwestern Union Co | 1433 | 57.8 | 4.85 | 62.6 | 3.17 | 0.0318 | 72.7 |
| 20071 | South-central Columbia Co | 3939 | 113 | 18.8 | 132 | 3.25 | 0.0325 | 67.9 |
| 25837 | Central Miller Co | 1155 | 55.0 | 1.46 | 56.5 | 3.40 | 0.0342 | 89.1 |
| 23829 | Southeastern Ashley Co | 3039 | 103 | 17.4 | 120 | 3.39 | 0.0339 | 59.7 |